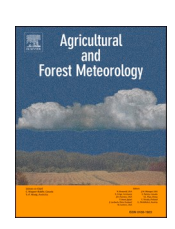
ELSEVIER

Contents lists available at ScienceDirect

### Agricultural and Forest Meteorology

journal homepage: www.elsevier.com/locate/agrformet





## Impact of interannual weather variation on ammonia emissions and concentrations in Germany

Xinrui Ge a,b,\*, Martijn Schaap b, Enrico Dammers b, Mark Shephard c, Wim de Vries a,d

- a Environmental Systems Analysis Group, Wageningen University, Wageningen, The Netherlands
- <sup>b</sup> Department of Climate, Air and Sustainability, TNO, Utrecht, The Netherlands
- <sup>c</sup> Environment Canada, Toronto, Ontario, Canada
- <sup>d</sup> Wageningen Environmental Research, Wageningen, The Netherlands

#### ARTICLE INFO

# Keywords: Ammonia Emission Emission fraction Spatial distribution Temporal distribution

#### ABSTRACT

Ammonia is one of the most impactful pollutants emitted from agricultural activities, harming human health and contributing to biodiversity loss. In ammonia emission inventories, the spatial distribution of annual emissions is mostly approximated by constant empirical emission fractions, which do not account for spatial variability, nor for temporal variability within a year or between years caused by weather variations. Besides, factors like manure properties, soil properties, and manure application techniques also lead to differences in the amount of ammonia emitted into the atmosphere. By not or only partly accounting for these factors, significant uncertainties are introduced into ammonia emission estimates at regional and national scales. In this study, we applied the empirical ALFAM2 model to derive spatially explicit slurry application emission fractions from cropland for use in the large-scale INTEGRATOR model, using the information on slurry properties (dry matter content and pH), manure application rate, application technique, incorporation time, air temperature, wind speed, and rainfall rate. In addition, the impact of weather on the ammonia emissions from animal housing and manure storage systems was included through a temperature-dependent scaling. We applied the method to investigate the year-to-year spatio-temporal variabilities of ammonia emissions and modeled concentrations across Germany from 2015 to 2018. Through the comparison with in situ measurements and satellite-derived observations, we studied how surface concentrations and total columns relate to local meteorology. We found that the spatio-temporal variability in emission fractions improves the ability to reproduce the interannual variability observed in ammonia concentration and total column measurements. This study shows that the developed approach to derive spatially explicit emission fractions can significantly improve ammonia emission modeling and is of great importance for studying the temporal variability between years.

#### 1. Introduction

Ammonia (NH<sub>3</sub>) is an important air pollutant, causing negative effects on human health and biodiversity at elevated concentrations (de Vries, 2021; Li et al., 2014). It reacts with sulphuric and nitric acid in the atmosphere, forming fine particulate matter (PM<sub>2.5</sub>), which leads to increased mortality related to lung disease (Giannadaki et al., 2018; Stokstad, 2014; Wang et al., 2017). Once deposited, it can lead to acidification and eutrophication in soils and surface waters, ultimately resulting in biodiversity loss in terrestrial and aquatic ecosystems (Erisman, 2021; Sutton et al., 2013). In many regions of the world, reactive nitrogen (Nr) deposition, whose essential composition is

ammonia, exceeds the critical loads of natural ecosystems (Forsius et al., 2021; Hettelingh et al., 2017). In Germany, the critical loads for eutrophication were estimated to have exceeded 70% of the ecosystem area in 2015 (Schaap et al., 2018). Since European countries have not managed to reduce ammonia emissions strongly, the negative impacts of ammonia emissions are not expected to decline substantially in the near future (European Environment Agency, 2019).

Agriculture is the dominant source of ammonia emission into the atmosphere, accounting for more than 90% of the emission total in the E. U. (Sintermann et al., 2012). Ammonia emissions from livestock manure and mineral fertilizer constitute a significant but variable proportion of reactive nitrogen loss (Amann et al., 2013; Hafner et al., 2019).

https://doi.org/10.1016/j.agrformet.2023.109432

<sup>\*</sup> Corresponding author.

E-mail address: jerry.ge@tno.nl (X. Ge).

Ammonia emissions from livestock manure, which includes manure (urine and feces) in animal houses, manure in storage systems, and manure applied to fields, contribute to nearly 80% of the total agricultural emissions at the European scale (EU27) (De Vries et al., 2011; Leip et al., 2015). Based on EMEP results in 2020, when EMEP revised the country-reported annual emission per sector of 2018, manure management (livestock housing and manure storage) for cattle, pigs, and poultry adds up to about 23%, 15%, and 5% of the annual emission total in Germany, respectively. In addition, the application of manure and mineral fertilizer to fields contributes to around 33% and 12% of the annual total (Umweltbundesamt, 2020).

Accurate estimates of ammonia emission are of great significance for Nr budgets at the field- or farm scale (Sintermann et al., 2012; Sonneveld et al., 2008), landscape scale (Cellier et al., 2011; de Vries et al., 2015), and national or continental scale (De Vries et al., 2011; Kros et al., 2018). The nitrogen flow approach is a common method to model annual ammonia emission within countries where emissions are calculated using emission fractions, which are the ratios between the emitted ammonia to the atmosphere and the total ammoniacal N (TAN) allocated in various agricultural sectors. This methodology has been adopted by Hutchings et al. (2001) for Denmark, Webb and Misselbrook (2004) for the U.K., Gac et al. (2007) for France, (Velthof et al., 2012) for the Netherlands, and by Dämmgen and Hutchings (2008) for Germany.

Many experiments on ammonia emission from livestock manure applied to fields have been conducted to develop or evaluate emission fractions (Sintermann et al., 2012; Webb and Misselbrook, 2004). The emission fractions used in the inventories are usually derived by experts averaging over time for each country, not considering either the spatial variability of meteorology or the differences in manure properties, application technique, and incorporation time. The need for including such temporal and spatial differences due to meteorology for accurately assessing ammonia emissions and deposition has been described in several publications (Ge et al., 2020; Jiang et al., 2021; Sommer et al., 2019; Truong et al., 2018; Van Damme et al., 2015). Neglecting such spatial and temporal differences affects the timing of manure and fertilizer application and the related emission fraction. The weather impact is more prominent on the more temporally variable emissions from manure and mineral fertilizer application than the less temporally variable emissions from animal housing and manure storage (Ge et al., 2020; Skjøth et al., 2011).

In assessing the temporal (intra-annual) and spatial variability using the INTEGRATOR model with the agricultural management model TIMELINES, Ge et al. (2020) identified overestimated ammonia emissions in Southern Germany and an underestimation in the country's north. The authors stipulated that this was likely due to using constant ammonia emission fractions for manure application, animal housing, and manure storage all over Germany. Furthermore, several studies have concluded that the currently available emission products do not correctly reflect the impact of inter- and intra-annual variability of ammonia emissions in terms of timing and amount (Backes et al., 2016; Hellsten et al., 2008; Hendriks et al., 2016; Skjøth et al., 2011), highlighting the need to improve the emission fractions for agricultural ammonia emission modeling.

The challenge of estimating field application emissions is formidable because of many influencing variables such as application techniques, manure properties, and the dependence on meteorological conditions. Several models have been developed to predict ammonia emissions from manure applied to fields (Congreves et al., 2016; Gericke et al., 2012; Misselbrook et al., 2005; Nicholson et al., 2013; Smith et al., 2009). Most of these models are empirical or process-based models that contain specific empirical components (Cuddington et al., 2013; Hafner et al., 2019), with each model type having its advantages and disadvantages. Process-based models can more accurately predict complicated responses under specific conditions (Hafner et al., 2019), while empirical models are generally easier to apply since they have fewer parameters and inputs. Process-based models such as the Volt'Air (Génermont and

Cellier, 1997) and Manure DNDC (Li et al., 2012) model by principle follow a more mechanistic approach. Volt'Air simulates the gaseous transfers between the soil and the lower atmosphere by dealing with nitrogen's physical and chemical equilibria, the soil surface's energy budget, and the transfers of heat, water, and solutes within the soil profile (Génermont and Cellier, 1997). The Manure DNDC model is based on thermodynamics and biogeochemical reaction kinetics, controlled by a group of environmental factors (such as temperature, soil moisture, and soil pH) (Li et al., 2012). In contrast, empirical models use relationships based on observed behavior in the field situation. For example, Huijsmans et al. (2018) utilized a logistic regression function to mimic the emission relative to discrete intervals after manure application. The ALFAM (Søgaard et al., 2002) and MANNER (Nicholson et al., 2013) models are two other examples of fully empirical models. They use a Michaelis-Menten function to predict the cumulative emissions simply because the shape of the function is similar to the observed pattern of emission over time. The semi-empirical dynamic model ALFAM2 (Hafner et al., 2019) finds a balance between the simplicity of empirical models and the more accurate representation of processes achieved with a process-based approach and accounts for many control variables. ALFAM2 is the successor of the widely used ALFAM model and is built on a two times larger database of ammonia emissions from field-application experiments than its predecessor. ALFAM2 accounts for the impacts of manure properties (dry matter, slurry pH), meteorology (air temperature, wind speed, and rainfall rate), and application techniques and incorporation time.

This paper aims to improve the spatial and temporal (interannual) variation of ammonia emissions within Germany by replacing countrydependent emission fractions with spatially-explicit gridded matrices using the ALFAM2 model approach. First, we describe the methodology of (1) the INTEGRATOR emission model, which generates spatially resolved N inputs in animal houses (excretion from urine and feces), manure storage systems, N applied to fields by manure and fertilizer application and by grazing; (2) the ALFAM2 model that predicts emission fractions of slurry manure application while accounting for variations in meteorology, manure properties, application techniques, incorporation time and application rates; (3) the chemistry transport model (CTM) LOTOS-EUROS which translates ammonia emission into atmospheric concentrations; and (4) satellite observations of ammonia total columns and in situ measurements of surface concentrations for validation. Subsequently, we evaluate the model performance by comparing modeled results and measurements over Germany from 2015 to 2018 to quantify the improved model's capability to reproduce the interannual variability of annual ammonia emission totals and the spatial and temporal variability of ammonia emissions. Finally, the results, potential shortcomings, and possible future methodological improvements are discussed.

#### 2. Methodology

A schematic overview of the modeling approach is presented in Fig. 1. The emission model consists of three modules, including a spatial allocator of manure, compost, and fertilizer N inputs, an emission fraction predictor of those inputs, and a temporal allocator of ammonia emissions. The spatial allocator produces the spatial distribution of N excretion in animal housing and manure system and on the field through manure and mineral fertilizer application and grazing using the INTE-GRATOR model. The emission fraction predictor derives emission fractions of slurry application with the ALFAM2 model and emission fractions of animal housing and manure storage using a temperaturebased scaling (TBS) algorithm. The INTEGRATOR outputs on grazing emissions and emissions from solid manure and mineral fertilizer application were kept as they were. It has to be noted that emissions from compost and digestate application are not included in INTE-GRATOR. However, the official German inventory started to include this sector in 2010. Therefore, we took the reported annual emission total of

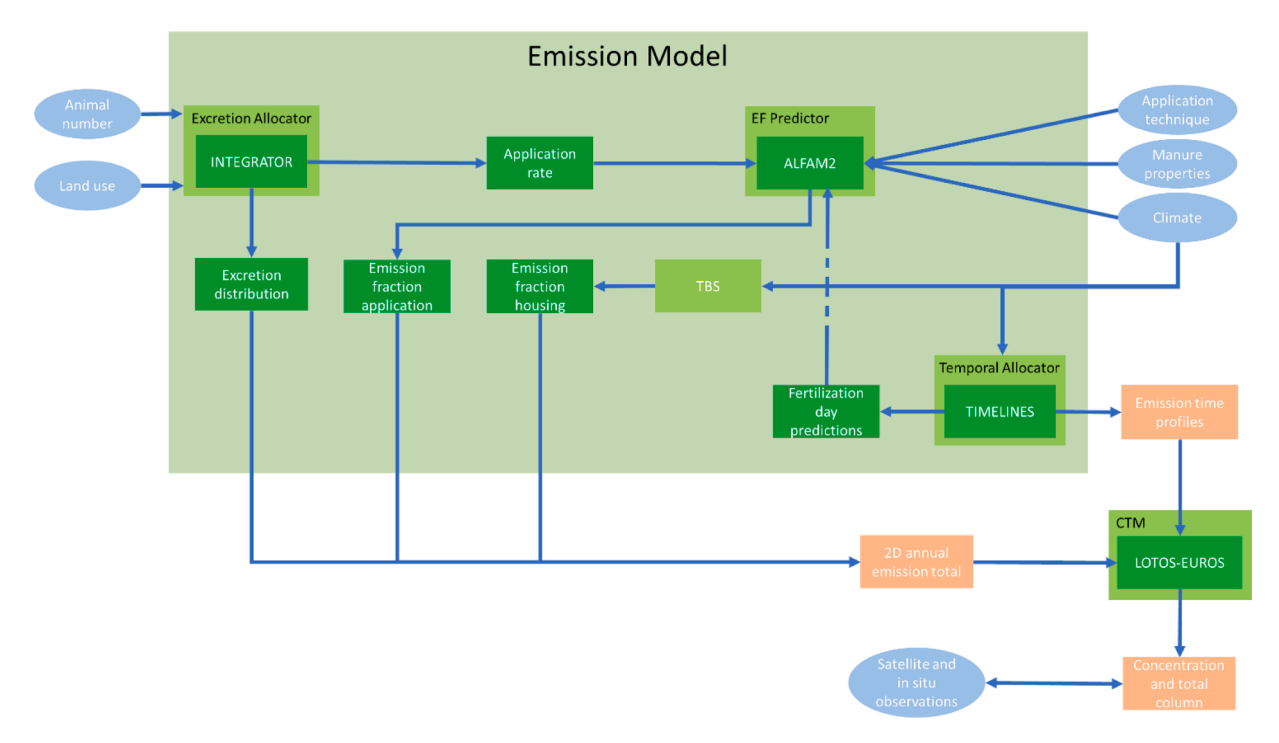


Fig. 1. Schematic overview of calculating the spatial and temporal distribution of ammonia emissions and validating by the comparison with measurements in this study.

this sector from European Monitoring and Evaluation Programme (EMEP) and used a top-down algorithm to spatially allocate the emission over Germany. The details can be found in the supplementary material. The temporal allocator creates emission time profiles that distribute gridded annual emissions in time, which also predicts fertilization dates that the emission fraction predictor requires.

The study area was set to be Germany due to data availability. Therefore, the spatial domain was  $5^{\circ}E-16^{\circ}E$  with a resolution of 0.1 degrees in longitude and  $46^{\circ}N-56^{\circ}N$  with a resolution of 0.05 degrees in latitude (approximately  $6\times 6~km^2$ ), corresponding to a domain size of 110 pixels by 200 pixels in longitude and latitude, respectively. For each year from 2015 to 2018, the 3D distribution of ammonia emissions (gridded annual emissions and emission time profiles) was then imported into the CTM LOTOS-EUROS to derive surface concentrations and total columns of ammonia. The simulated values were evaluated with remote sensing observations and in situ measurements.

#### 2.1. Spatial allocator of manure, compost, and fertilizer inputs

#### 2.1.1. The INTEGRATOR model

The INTEGRATOR model is a static N cycling model that can assess N emissions from housing, manure storage systems, and the soil (due to manure and mineral fertilizer application) in response to European-scale changes in land use, land management, and climate (De Vries et al., 2011). INTEGRATOR estimates emissions in NitroEurope Classification Units (NCUs), which are multi-part polygons composed of 1 km  $\times$  1 km grid cells in the ETRS89/LAEA Europe coordinate system (for a detailed description of NCU, we refer to Ge et al. (2020).

The emission model starts with calculating total N excretion by multiplying the number of animals at the NCU level with the N excretion rate per animal per country for various animal categories (Kros et al., 2012). The total manure production is derived by subtracting gaseous emissions and leaching in housing and manure storage systems from the N excretion. The N excreted within housing systems is the multiplication of N manure excretion and the housing contribution fraction, while the N excreted from grazing on land is obtained by subtracting N excreted in housing systems from total N manure excretion. Manure is then

allocated over grassland and arable crop groups using various allocation rules. Manure produced by grazing animals and in housing systems by sheep and goats all enter grassland. A fraction is applied to arable land for other manure, and the remaining fraction is applied to grassland/fodder crops. For the distribution of manure application on arable land, we distinguish three arable crop groups with (i) a relatively high use of manure (sugar beet, barley, rape, and soft wheat), (ii) an intermediate use of manure (potatoes, durum wheat, rye, oats, grain maize, other cereals including triticale, and sunflower), and (iii) low use of manure (fruits, oil crops, grapes, and other crops) using weighing, based on Velthof et al. (2009). Finally, no manure is allocated to dry pulses and rice, fiber crops, other root crops, and vegetables. The amount of mineral fertilizer needed is then estimated with an N-balanced approach, which we refer to Ge et al. (2020) for more details.

After the N excretion distribution of housing, grazing, and manure and fertilizer application is obtained, the gaseous emission of each category is derived by the multiplication with the emission fraction per housing system, for grazing, and manure and fertilizer application, respectively (De Vries et al., 2020; Kros et al., 2012). The spatial allocator in this study is the subcomponent of INTEGRATOR that produces the N excretion distribution before multiplying emission fractions. The NCU-level N excretion from the spatial allocator was resampled to the grid cells in this paper. Furthermore, N from manure and mineral fertilizer application on the fields was reallocated to the corresponding crops and grassland based on the crop map.

#### 2.1.2. Input data

The input data of INTEGRATOR are classified into three categories: biophysical data (soil, land use, and climatic data), agricultural activity data (animal numbers and N excretion rates), and emission information (fractions of N emission, leaching, and runoff). The version of INTEGRATOR in this study was developed for the year 2010 and used by Ge et al. (2020) to improve the spatial details of ammonia emission. Since this study focused on 2015 – 2018, the input data on animal numbers and land use were revised.

#### 2.1.3. Animal numbers

The livestock data in INTEGRATOR (version 2010) were obtained from the FAO database at the country level, using Common Agricultural Policy Regionalised Impact analysis (CAPRI) data for distribution at the NUTS2 level. The data on livestock numbers of various animal categories at the NUTS2 level were downscaled to a 1 km imes 1 km resolution using expert-based judgment with spatial data sources on land use, slope, altitude, and soil characteristics influencing the livestock carrying capacity (Neumann et al., 2009). However, the animal number data officially reported to EMEP from the German inventory differ substantially from those in FAO used by INTEGRATOR, especially after 2010 (Haenel et al., 2020). There are several reasons for the diverging animal numbers of the two datasets. For cattle (including buffalo), FAOSTAT contains the data of the May census in the years 2011 - 2013, while German inventory uses the data of the November census as required by E.U. regulations. The FAOSTAT animal numbers for cattle only agree with the official German data after 2013. The FAOSTAT numbers of pigs, sheep, and goats are generally not comparable with the number in the German inventory. Because in the German inventory, the number of suckling piglets (i.e., piglets weighing less than 8 kg) is subtracted, the number of sheep number was revised in 2010, and the number of goats was linearly interpolated to fill in missing values (Haenel et al., 2020). Therefore, we adjusted the animal numbers in INTEGRATOR for 2010 to align them with those in the German inventory for the years 2015-2018,

$$N(ani, INT, NUTS)_{2015-2018} = N(ani, INT, NUTS)_{2010} \times \frac{N(ani, INT, state)_{2015-2018}}{N(ani, INT, state)_{2010}}$$
(1)

where  $N(ani,INT,state)_{2015-2018}$  is the reported animal numbers per animal type per federal state in Germany averaged over the years 2015-2018 and  $N(ani,INT,state)_{2010}$  is the calculated animal numbers per animal type per state in Germany averaged for 2010 in INTEGRATOR, based on the NUTS-level data.

#### 2.1.4. Land use

The standard land use input in INTEGRATOR is the total area of each arable crop or grassland for each NCU based on the year 2010, requiring an update for 2015 – 2018. Thus, we used an updated map of crop and land cover classes for Germany in 2016 based on the crop map developed by Griffiths et al. (2019), who integrated multitemporal multispectral Sentinel-2 and Landsat reflectance data and subsequently generated equidistant, dense, and intra-annual composite time series to provide this national scale map. We used the crop raster map to derive crop areas per NCU for the five years to control the number of variables, assuming that crop rotation in a grid remains semi-constant over the years.

#### 2.2. Temporal allocator of ammonia emissions

The usual approach to characterizing the temporal variability in  $NH_3$  emissions is to use time profiles that distribute the annual emission total in a grid cell over a year. Ge et al. (2020) explicitly described the temporal allocation of  $NH_3$  emissions from manure and fertilizer application, grazing, animal housing, and manure storage based on the concepts of Skjøth et al. (2004), Gyldenkærne et al. (2005). The temporal allocator in this study used TIMELINES (Hutchings et al., 2012) to predict the fertilization days for the years between 2015 and 2018 by introducing a thermal time approach. Thermal time is the sum of the positive differences between the daily mean air temperature and a base temperature (0 degrees Celcius). Starting from 1 January, as soon as thermal time on Julian day t reaches the reference thermal time for sowing (or harvesting), it is considered that sowing (or harvesting) occurs on Julian day t. Field operations like manure and mineral fertilizer applications are related to it. The fertilization day predictions were used to construct

the time profiles of ammonia emissions from manure and fertilizer application. Regarding the details of the temporal allocator of ammonia emission, we refer to Ge et al. (2020). The fertilization days were also taken into account when we generated meteorological condictions for emission fraction calculations in ALFAM2, which will be elaborated later

#### 2.3. Emission fraction of manure slurry application

Originally, the obtained N distribution in housing systems and on the field is then combined with the corresponding  $\rm NH_3\text{-}N$  emission fractions in INTEGRATOR, which depend on the animal category, manure type (liquid/solid), and the degree of implementation of emission-reducing techniques per country. In this study, the INTEGRATOR outputs for N slurry application rates were combined with information on meteorology and manure properties for use in the second module (the emission fraction predictor) to calculate the emission fraction of slurry application using the ALFAM2 model.

#### 2.3.1. The ALFAM2 model

The ALFAM2 model simulates the behavior of applied total ammoniacal nitrogen (TAN, kg ha<sup>-1</sup>) over time, based on Chantigny et al. (2004). After the slurry is applied to land, TAN is immediately partitioned between two pools: a "fast" pool representing slurry in direct contact with the atmosphere, and a "slow" pool representing fractions less available for emission due to slurry infiltration (Chantigny et al., 2004; Sommer et al., 2004), adsorption of ammonium (NH<sub>4</sub>+) on cation exchange sites (Pelster et al., 2019), crust formation (Thompson et al., 1990), injection (Webb et al., 2010), or incorporation (Huijsmans, 2003). ALFAM2 parameters value on partitioning and transfer rates, quantifying the effects of slurry application, were estimated from an extensive data set of emissions from cattle and pig slurry (490 field plots in 6 countries from the ALFAM2 database). An analysis of a large subset of the ALFAM2 database showed that most total measured ammonia emission from slurry application generally occurs within 72 hours (Hafner et al., 2018). Consequently, the ALFAM2 model is restricted to a maximum duration of 72 hours (3 days) after slurry application to allow parameter estimation. Therefore, we calculated emission fractions as the relative accumulated emission (ratio between N emitted as ammonia and TAN applied) at the 72<sup>nd</sup> hour.

Fig. 2 shows an example of accumulative fractional emission calculated with ALFAM2 for different surface temperature conditions to inspect the impact of temperature. The x-axis represents the number of hours after slurry application (72 hours maximum), and the y-axis is the accumulative fractional emission. Three surface temperature (20, 15, and 10 degrees Celsius) conditions were studied, while other variables remained the same. In this experiment, the TAN was set to be 40 g/kg, and the dry matter of manure is 8% the application method is broadcast with an incorporation time of 2 hours after application. One can see that the largest share of the ammonia emission takes place within the first 6 hours after application, and then it gradually increases at a much lower rate. Furthermore, higher temperature results in higher N loss to the atmosphere in the form of ammonia. The emission fractions for these three temperature scenarios are around 0.40, 0.32, and 0.25, respectively, illustrating the importance of meteorological conditions during application activities.

#### 2.3.2. Input data

ALFAM2 input data include slurry dry matter and pH, application rate, application method and incorporation time, air temperature, wind speed, and rainfall rate. Consequently, these variables were included to derive a spatially explicit and dynamic emission fraction product.

#### 2.3.3. Manure properties and application rate

Manure properties accounted for in ALFAM2 include slurry dry matter content and pH. The dry matter values of cattle, pig, and poultry

#### Accumulative relative emission as function of time under different temperature conditions

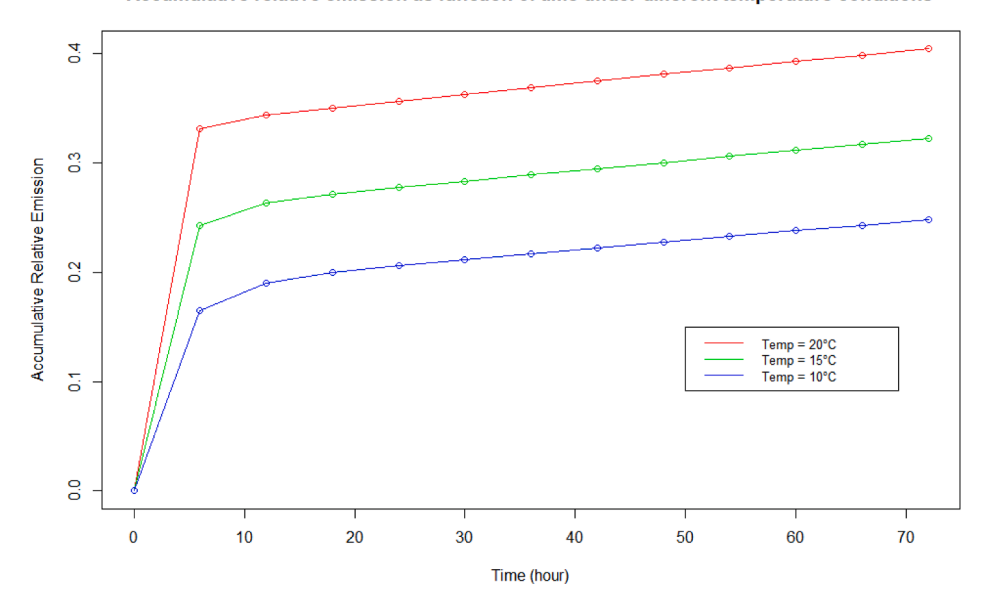


Fig. 2. Accumulative relative emission as a function of time under average temperature conditions (20, 15, and 10 degrees Celsius).

liquid manure were reported averages of different types of manure composition used in INTEGRATOR from the RAMIRAN network (Menzi et al., 2002). The dry matter values of cattle and pig slurry were set to 67 g/kg and 52 g/kg, respectively. The pH of cattle and pig slurry were both set at 7.9 based on Joubin (2018) and Martínez-Suller et al. (2010). The spatial distribution of the slurry application rate was obtained from the excretion allocator described previously.

#### 2.3.4. Application method and incorporation time

Data on the slurry application method in Germany, which differentiates broadcasting, trailing hose, trailing shoe, slot method, cultivator, and injection, were derived from a survey in 2015, namely Wirtschaftsdünger tierischer Herkunft in landwirtschaftlichen Betrieben/Agrarstrukturerhebung, by the Federal Statistical Office of Germany (Statistisches Bundesamt). This survey gives the area of cropland and grassland on which each application technique was applied at the federal state (Bundesland) level. For arable land, the areas also include a distinction in incorporation time, i.e., no incorporation, incorporation right after application (incorporation time 0), incorporation within one hour (incorporation time <1h), and after one hour (incorporation time > 1h) following application. Since it is unknown which application

method is applied on individual fields within a given federal state, we calculated all possible emission fractions for all methods and incorporation options mentioned in the survey with ALFAM2. We then used weighing factors, namely the area per application method per incorporation time divided by the total area, to derive weighted means of emission fractions. An overview of the area percentage of the application techniques on arable land at the state level is given in Table 1.

#### 2.3.5. Meteorology

The ALFAM2 model requires air temperature, wind speed, and rainfall rate as meteorological input for emission fraction prediction. We obtained these variables from the ERA5-Land datasets in the Copernicus Climate Data Store (https://cds.climate.copernicus.eu/cdsapp#!/dataset/reanalysis-era5-land). The spatial resolution of the products is 0.1 by 0.1 degrees; thus, it was resampled to the grid in this study. ERA5-Land is a reanalysis dataset providing land variables over several decades at an enhanced resolution compared to ERA5. As previously described, we predicted the fertilization days for each crop from the temporal allocator and calculated the mean air temperature, wind speed, and rainfall rate for the five days before and after the predicted fertilization days. These were the inputs for ALFAM2 so that the data derived could better

Table 1
Fraction of different application methods and incorporation time applied on arable land per German federal state.

Application technique	Broadc	ast			Trailing	g hose			Trailing	g shoe			Slot inj	ection		
Incorporation time	/	0	<1h	>1h	/	0	<1h	>1h	/	0	<1h	>1h	/	0	<1h	>1h
Baden-Wurttemberg	0.401	0.033	0.116	0.122	0.165	0.008	0.027	0.029	0.034	0.001	0.005	0.005	0.020	0.004	0.015	0.016
Bayern	0.333	0.095	0.142	0.092	0.028	0.007	0.010	0.007	0.103	0.021	0.032	0.021	0.040	0.020	0.030	0.019
Berlin	1.000	0.000	0.000	0.000	0.000	0.000	0.000	0.000	0.000	0.000	0.000	0.000	0.000	0.000	0.000	0.000
Brandenburg	0.035	0.054	0.058	0.043	0.211	0.104	0.112	0.083	0.024	0.007	0.007	0.005	0.038	0.076	0.082	0.061
Bremen	0.366	0.063	0.091	0.099	0.232	0.010	0.014	0.015	0.072	0.003	0.004	0.005	0.025	0.000	0.000	0.000
Hamburg	0.030	0.055	0.080	0.213	0.257	0.032	0.046	0.124	0.032	0.004	0.006	0.015	0.020	0.014	0.020	0.053
Hessen	0.345	0.036	0.175	0.188	0.113	0.006	0.030	0.032	0.017	0.002	0.008	0.008	0.011	0.003	0.013	0.014
Mecklenburg-	0.093	0.053	0.085	0.065	0.276	0.063	0.101	0.078	0.008	0.002	0.003	0.003	0.020	0.039	0.062	0.048
Vorpommern																
Niedersachsen	0.165	0.053	0.117	0.060	0.232	0.040	0.088	0.045	0.057	0.008	0.018	0.009	0.020	0.020	0.044	0.023
Nordrhein-Westfalen	0.176	0.030	0.097	0.038	0.380	0.027	0.089	0.035	0.039	0.004	0.012	0.005	0.020	0.009	0.029	0.011
Rheinland-Pfalz	0.367	0.036	0.203	0.154	0.094	0.006	0.033	0.025	0.019	0.001	0.005	0.003	0.017	0.004	0.019	0.015
Saarland	0.327	0.014	0.333	0.185	0.053	0.001	0.027	0.015	0.000	0.000	0.005	0.003	0.031	0.000	0.004	0.002
Sachsen	0.028	0.080	0.021	0.017	0.077	0.089	0.023	0.019	0.025	0.008	0.002	0.002	0.098	0.347	0.090	0.075
Sachsen-Anhalt	0.042	0.058	0.029	0.038	0.213	0.110	0.055	0.072	0.030	0.011	0.006	0.007	0.038	0.135	0.068	0.088
Schleswig-Holstein	0.270	0.043	0.154	0.097	0.248	0.014	0.049	0.031	0.014	0.001	0.003	0.002	0.012	0.009	0.032	0.020
Thuringen	0.026	0.030	0.007	0.006	0.242	0.100	0.024	0.018	0.016	0.004	0.001	0.001	0.099	0.298	0.073	0.055

represent the weather condition during fertilization.

The weighted mean of emission fractions at a location was calculated as:

$$EF(x,y) = \sum \frac{Area_{AT,T_{incorp}}(x,y)}{Area_{um}(x,y)} EF_{AT,T_{incorp}}(x,y)$$
 (2)

where (x, y) is the coordinates of a location.  $Area_{AT,T_{Incop}}(x,y)$  is the area of arable crops or grassland on which application technique AT with a given incorporation time  $T_{incop}$  is used in the German state where (x,y) is located,  $Area_{sum}(x,y)$  is the area sum of arable crops or grassland surveyed in the same German state,  $EF_{AT,T_{incop}}(x,y)$  is the predicted emission fraction of application technique AT with incorporation time  $T_{incop}$  from the ALFAM2 model, calculated as:

$$EF_{AT,T_{incorp}}(x,y) = f_{ALFAM2}\left(AT,T_{incrop},T(x,y),W(x,y),P(x,y),DM,pH,R_{app}(x,y)\right)$$
(3)

where AT,  $T_{incrop}$ , T(x,y), W(x,y), P(x,y), DM, pH,  $R_{app}(x,y)$  are the application method, incorporation time, temperature, wind speed, precipitation rate, manure dry matter, manure pH, and application rate at a given location, respectively.

#### 2.4. Emission fraction of animal housing and manure storage

We used a temperature-based scaling algorithm to derive the spatial and interannual variability of animal housing and manure storage emission fractions. Skjøth et al. (2011) and Gyldenkærne et al. (2005) describe the emission pattern from animal housing and manure storage as below:

$$\begin{cases}
Fkt_i = E_i(x, y) \times (T_i(x, y))^{0.89}, \ T_i(x, y) \ge T_{boundary} \\
T_i(x, y) = \begin{cases}
18 + 0.77 \times (T(x, y) - 12.5), \ Houses \ with \ forced \ ventilation \\
T(x, y) + 3, \ Open \ animal \ houses
\end{cases}$$

$$T(x, y), \ Manure \ storage$$
(4)

where i refers to the index (1-3) of houses with forced ventilation, open animal houses, and manure storage, respectively. x, y are the coordinates of the emission grid.  $E_i(x,y)$  represents the emission for the corresponding agricultural sector within the grid cell.  $T_i(x,y)$  is the temperature function. T(x,y) is the 2-meter temperature at the given location. Open houses and manure storage have almost the same emission pattern, except that the indoor temperature in open houses is 3 degrees higher than the outside temperature used for manure storage (Gyldenkærne et al., 2005).  $T_{boundary}$  represents lower boundary condition for temperature in animal housing and manure storage, below which emission is set to a constant level, and they are 18, 4, and 1 degree for houses with forced ventilation, open animal houses, and manure storage, respectively.

The concept of temperature-based scaling is to calculate the time profile of the three categories (insulated housing, open housing, and manure storage), using the mean temperature between 2015 and 2018 to represent the averaged pattern of ammonia emission spatially and between years as the base. Subsequently, we used the temperature time series of each year and calculated the deviations from the base at every grid cell, aiming to introduce the variability of the emission fraction based on the deviations.

First, we calculated the spatial distribution of the base emission fraction  $EF_{i,\ base}(x,y)$ :

$$EF_{i,base}(x,y) = \frac{Fkt'_{i,mean}(x,y)}{mean(Fkt'_{i,mean})} \times EF_{i,int}$$
(5)

where  $Fkt'_{i,mean}(x,y)$  is the mean of the function values calculated by the 4-year mean temperature above  $T_{boundary}$  at a given location,

 $mean(Fkt_{i,mean}')$  is the mean of  $Fkt_{i,mean}'(x,y)$ ,  $EF_{i,int}$  is the emission fraction introduced in INTEGRATOR. This was under the assumption that the static country-dependent emission fractions represent the emission level with mean temperature conditions over the four years. Subsequently, the gridded emission fraction of housing and storage in each year was calculated as:

$$EF(x,y) = EF_{i,base}(x,y) \times \sum_{t=1}^{n} \frac{Fkt_i(x,y,t)}{Fkt_{i,mean}(x,y,t)}$$
(6)

where  $Fkt_i(x,y,t)$  is the function value at the hourly time step t in a year at a given location using the original temperature data,  $Fkt_{i,mean}(x,y,t)$  is the function value at time step t at a given location using the 4-year mean temperature.

#### 2.5. Validation of model estimates to measurements

To validate the emission estimates, we imported the gridded annual emissions and time profiles into LOTOS-EUROS to derive surface concentration and total column which were compared with in situ measurement and satellite observation, respectively.

#### 2.5.1. The LOTOS-EUROS model

The LOTOS-EUROS model is an Eulerian chemistry transport model that simulates air pollution in the lower troposphere (Manders et al., 2017; Schaap et al., 2012, 2008). In this paper, the spatial resolution of LOTOS-EUROS was set to be the same as the emission product, namely 0.1° in longitude and 0.05° in latitude. In the vertical, we applied the well-mixed dynamic boundary layer concept. There are four dynamic layers and a surface layer. The lowest dynamic layer is the mixing layer, followed by three reservoir layers. The model's physical processes include advection, diffusion, dry and wet deposition, chemistry reaction, and sedimentation. LOTOS-EUROS uses a set of temporal factors (monthly, daily, and hourly) to break down annual total emissions into hourly emissions. LOTOS-EUROS has been used for a wide range of applications supporting scientific research. It is used for daily operational air quality forecasts over Europe (Marécal et al., 2015) and the Netherlands (Hendriks et al., 2013), as well as for daily forecasts of dust concentrations over North Africa (Dominguez-Rodriguez et al., 2020), and the forecast of dust storms in China (Jin et al., 2021).

The LOTOS-EUROS CTM was used to simulate surface concentrations and total columns from the emission products. After replacing the gridded annual ammonia emission input with the newly developed emission distribution and replacing the fixed simplified temporal factors with updated spatially explicit time profiles, the improvements can be evaluated by comparing modeling results with in situ measurements and satellite observations.

Three LOTOS-EUROS simulations with a 4-year duration were performed in this study: 1) the base scenario (referred to as BASE in this paper) using the gridded annual emissions from the INTEGRATOR output that was scaled by reported country totals (as in Ge et al. (2020)) and the default simplified hourly emission time profile setting in LOTOS-EUROS; 2) a second reference case (referred to as TIME) which uses the same gridded annual emissions in BASE and the dynamic and a spatially explicit time profile developed with the method from Ge et al. (2020); 3) the test case (referred to as SPACETIME) using the gridded N distribution from INTEGRATOR combined with meteorology-dependent emission fractions for slurry application, animal housing and manure storage with ALFAM2 and the same activity time profile as in TIME. An overview of the three scenarios is listed in Table 2. By comparing the BASE and TIME scenarios, the impact of dynamic time profiles can be determined since meteorological conditions affect the timing of fertilization practices and thereby the intra-annual time distribution of ammonia emission (Ge et al. (2020)). By comparing the TIME and SPACETIME scenarios, the improvement introduced by the updated emission fractions in this study can be quantified.

**Table 2**An overview of emission input the three model runs in this study.

Scenario	Gridded annual emission	Time profile
BASE	INTEGRATOR output with constant emission fractions and scaled with national totals per sector (Ge et al., 2020)	Country-dependent, fixed time profile in LOTOS-EUROS
TIME	INTEGRATOR output with constant emission fractions and scaled with national totals per sector (Ge et al., 2020)	Spatially explicit activity time profile, varying per year depending on meteorological conditions (Ge et al., 2020)
SPACETIME	INTEGRATOR output with meteorology-dependent spatially explicit emission fractions	As above, the timing remains the same but the amplitude is adjusted due to different gridded emissions induced by the meteorology-dependent emission fractions the timing

#### 2.5.2. Satellite observations of ammonia total columns

To evaluate the modeled distributions we used satellite observations. The Cross-track Infrared Sounder (CrIS) instrument is a Fourier Transform Spectrometer (FTS) launched by the U.S. NOAA/NASA on both the Suomi National Polar-orbiting Partnership (S-NPP) satellite on 28 October 2011 and the NOAA-20 satellite on 29 November 2017 (Shephard et al., 2020; Shephard and Cady-Pereira, 2015). CrIS is an across-track scanning hyperspectral infrared instrument in a sun-synchronous orbit (824 km) with a 2200 km swath width (±50°) with the total angular field of view consisting of a  $3 \times 3$  array of circular pixels of 14 km diameter each (nadir spatial resolution). CrIS provides soundings of the atmosphere over three wavelength bands in the infrared with a spectral resolution of 0.625 cm<sup>-1</sup>. The wavelength range 9.14–15.38  $\mu$ m (650–1095 cm<sup>-1</sup>) is used to retrieve ammonia, as the main ammonia infrared absorbing band lies in this spectral region, with the strongest absorption features between 960 and 970 cm-1 (Shephard and Cady-Pereira, 2015).

The CrIS has some advantages in contrast to other instruments. First, it has dense global coverage. In addition, it has improved sensitivity in the boundary layer due to the low spectral noise of  $\sim$ 0.04 K at 280K (4 times lower than IASI (Clarisse et al., 2009; Van Damme et al., 2017)) in the ammonia spectral region (Zavyalov et al., 2013). Therefore, it has the potential to detect smaller ammonia concentrations than are currently possible with IASI. Furthermore, the early afternoon overpass (a mean local daytime overpass time of 13:30 in the ascending node) coincides with higher thermal contrast (difference between the surface and air temperature), which is a more favorable measurement condition for infrared instruments (Shephard et al., 2020). Lastly, the CrIS fast physical retrieval (Shephard and Cady-Pereira, 2015) provides vertical sensitivity and robust and straightforward retrieval error estimate based on the retrieval input parameter. The CrIS averaging kernel usually has a maximum between 680 hPa and 850 hPa depending on the local conditions and a significant decrease near the surface since the instrument has reduced sensitivity near the surface. We only used the simulated output closest to the measurements in space and time to harmonize modeled and measured total columns during comparison. Furthermore, we applied the linearized averaging kernel (Cao et al., 2022) of each CrIS observation to the corresponding model result when calculating total columns LOTOS-EUROS three-dimensional from the concentrations.

The CrIS v1.6.1 data product was downloaded from https://hpfx.collab.science.gc.ca/~mas001/satellite\_ext/cris/snpp/nh3/. Daytime observations between January 2015 and December 2018 were used for this study. Furthermore, only observations with a quality flag of 3 were selected. The measurements with signal-to-noise ratio >2, degrees of freedom >0.8, and thermal contrast >-2 K were selected to filter out anomalous values due to thin clouds, very cold surfaces, and observations with low information content (Shephard et al., 2020).

It has to be noted that there is a background level ammonia total column from CrIS observations. Shephard and Cady-Pereira (2015) determined the minimum ammonia detection limit of CrIS, which is caused by the relatively weak atmospheric spectral signal of ammonia compared with the background infrared signal. The minimum detection limit was assumed to be where SNR is between 1 and 2. When ammonia concentration is low, the infrared signal will also be small. The CrIS instrument has relatively lower minimum detection levels, and here a more conservative limit of 0.9 ppb is assumed to cover most of the conditions found in the observations (Shephard and Cady-Pereira, 2015). Assuming that 1 ppb is equal to a total column  $(2\pm1)\times$  $10^{15} \text{molec/cm}^2$ , so the lower limits of CrIS was set to be  $(1.8 \pm 0.9) \times$ 10<sup>15</sup>molec/cm<sup>2</sup> (Dammers et al., 2019). However, the threshold used in this paper to exclude the background constant total column is much higher  $(1 \times 10^{16} molec/cm^2)$ , below which a measurement was omitted, because we wanted to focus on the agriculturally active regions.

#### 2.5.3. In situ measurements of ammonia surface concentrations

In addition to satellite observations of total columns, there are surface concentration measurements that were conducted by the Umweltbundesamt (UBA) research foundation. UBA sets up monitoring stations, providing information on air pollutants to governments and the public. It measures species, including ammonia and greenhouse gases, essential for improving air quality and climate change knowledge. The UBA also collects data from the network of the German federal states. In this study, the in situ data is available for 2015 – 2018 with weekly temporal resolution.

## 2.5.4. Calculation of the mean surface concentrations and total columns during peak periods

Emissions from slurry application and animal housing in single grid cells are expected to differentiate after applying the new emission fractions. However, the change is disaggregated into hourly time series using the time profiles, making it less noticeable in an absolute sense and more challenging to detect the improvement brought by our developments. Since the paper aims to reproduce the emission trend brought on by meteorology, we can validate it by analyzing if the new model can reproduce the trends illustrated by the sensitivity of surface concentration and total columns to temperature. This is because the temperature is the most decisive factor for the emission potential since other factors such as application methods and manure properties were kept the same at the state level every year.

The in situ measurements have extensive temporal coverage but low spatial representativeness, while the satellite observations have large spatial coverage but limited temporal continuity due to measurement quality. Therefore, it is more reasonable to look at the ammonia level in a larger region instead of a single location to illustrate the improvements of the new methodology. The UBA measurements and CrIS observations usually show three ammonia level peaks in a year. These are a prominent peak in the time block I between Julian Day 77 and 137 (caused by the first spring fertilization) and a lower peak in the time block II between Julian Day 147 and 197 (due to the second spring fertilization), and a flatter and more subtle peak (representing summer application and housing/storage emissions) in the time block III between Julian Day 207 and 277. Therefore, we calculated the mean surface concentrations and total columns of the three time blocks for each state in the four years and studied the trends against the mean temperature of the corresponding time blocks and states. To identify the models' capability to simulate concentrations in response to temperature, we conducted a comparison between simulated and measured slopes of the response of surface concentration to temperature in the three periods. It has to be noted that during the comparison of surface concentration trend, there was a distinguishment between coastal stations (which only exist in Mecklenburg-Vorpommern and Niedersachsen) and in-land stations. The ammonia levels measured by coastal stations demonstrated

significantly fluctuating patterns due to their unique locations with strong wind and humidity and ammonia's high reactive properties. As a result, they were excluded during the validation.

#### 3. Results

#### 3.1. Annual emission totals and time series per sector

The emission totals for Germany calculated with the updated emission fractions as categorized in the EMEP database for years from 2015 to 2018 are compared with the ones with the static emission fractions in Table 3. The magnitudes of the estimated annual emission totals using weather-dependent emission fractions were only slightly different from those estimated using the original (constant) emission fractions in the INTEGRATOR model for animal housing and manure storage. Some newly estimated emission totals are quite different from the original ones, the deviation is especially apparent for manure application emissions, which increased by 22% (2016) and 29% (2018). The interannual variability of manure application emissions was also induced, even though it was rather limited with the largest relative difference of 6.4% between 2016 and 2018. On the contrary, the emissions from other livestock management sources (animal housing and manure storage) did not change significantly, which was within our expectations. The temperature-based scaling impacted the spatial variation of emissions more than the absolute totals because it was based on the static emission fractions used in INTEGRATOR, representing the averaged ammonia level per sector over the whole country. The largest interannual variation is cattle housing and storage emissions, which is 8.7% between 2016 and 2018.

By comparing the modeled emissions in Table 3 with the officially reported data in Table 4, one can see that the updated emissions are more aligned with the official data for fertilizer and manure application but less for cattle housing. For other sectors, the results are rather similar. The absolute relative difference in manure application emissions between this study and official data decreased from around 17% to within 10% (1.58% in 2016). In addition, manure housing and storage emissions differ quite dramatically for both the original and updated emissions, especially for cattle (around -26%) and pigs (around +30%). The deviations between reported and modeled emissions from cattle and pig housing and manure storage are caused mainly by excretion rates and emission fractions used in INTEGRATOR. After adding reported emissions from compost and digestate application into INTEGRATOR results, the relative difference between the reported country totals and the updated estimated totals has been reduced except for 2018.

There are also deviations in interannual trends between the reported and newly updated emission estimates. The effect of including temperature change caused a slight increase in the updated modeled emissions in all sectors from 2016 to 2018, with the last increase from manure application (from 203 kton to 216 kton). On the contrary, the reported numbers were either constant or indicated a slight decline (for cattle housing and mineral fertilizer application) during these years, even

**Table 3**Comparison of reported emission total per sector and corresponding estimated emission total using the original emission fraction in INTEGRATOR.

EMEP category		on using v n (kiloton	Constant EF		
	2015	2016	2017	2018	2015-2018
Cattle housing and storage	105	103	104	112	106
Pig housing and storage	121	122	121	127	123
Poultry housing and storage	30	30	30	31	31
Manure application	209	203	213	216	167
Mineral fertilizer application	100	100	100	101	100
Grazing	25	25	25	26	24
Compost application	56	56	55	56	56
Total	648	640	649	669	607

Table 4

Annual ammonia emission total per sector officially reported by Germany between 2015 and 2018

EMEP category	Reported emission (kiloton)							
	2015	2016	2017	2018				
Cattle housing and storage	152	150	148	146				
Pig housing and storage	94	93	94	91				
Poultry housing and storage	30	30	30	31				
Manure application	201	200	199	197				
Mineral fertilizer application	105	100	94	74				
Grazing	9	9	9	9				
Compost application	56	56	55	56				
Total	647	639	630	602				

though the extent is rather low (from 201 kton to 197 kton). The total uncertainty of reported emissions from German agriculture is 10.7%, which is primarily determined by the uncertainties in the manure management of dairy cows and fattening pigs, the application of mineral fertilizers, and the spreading of animal manures (Rösemann et al., 2021). The difference between the updated emission estimates and the reported data lies within the uncertainties.

An example of the weekly time series of ammonia emission from animal houses, manure storage, and fertilization on various crops from 2015 to 2018 is given in Fig. 3. Fig. 3(top) and (bottom) represent the scenarios TIME and SPACETIME which use the INTEGRATOR annual distribution and the emission estimates with the original and updated emission fractions, respectively. The most noticeable feature in both time series is the seasonal cycle, with ammonia concentrations being at peaks in the warm growing season and at much lower levels during the colder period from late autumn to early spring. There are multiple peaks in concentration amounts during the growing season that can be associated with emissions from fertilization on various crops in spring, emissions from animal housing following increasing temperatures, and emissions from fertilization on winter crops. For both time series, cattle housing emissions experienced a rise from January to summer, followed by a decline till winter. In contrast, pig and poultry housing emissions are more constant over the years. This is because cattle houses are mostly open, while pig and poultry houses are partly or completely closed with forced ventilation. As a result, cattle housing is more sensitive to temperature changes, while the other housings keep a more constant level regardless of the temperature variability.

As expected, the application emission level fluctuates more when using weather-dependent emission fractions (Fig. 3(bottom)) than with constant emission fractions (Fig. 3(top)) with the most obvious change for fodder maize, since the difference between the original and updated emission fractions of manure application were largest on fodder maize. Fig. 3(top) shows that the emission peak is the highest in 2017 (slightly under 1.4 Gg/week) and the lowest in 2016, even though the difference is very small. However, in Fig. 3(bottom), the peak in 2018 is about at the same level as in 2017, being the highest among the years. This is because the temperature in 2018 is on average higher than that in 2017, which resulted in higher emission fractions from slurry manure application.

## 3.2. Simulated and measured surface concentrations in response to temperature

For the three above-mentioned time blocks of 2015 – 2018, we calculated the mean concentrations and the mean temperature for each state. Then, linear regression was performed per time block for each scenario and slopes of the linear regression between the response of surface concentration to temperature were derived. Fig. 4 compares the slopes (temp-sfcconc coefficient) in all German states during the three time blocks (from up to bottom is the time block I, II, III) derived from the measurements and the three simulation runs (from left to right is the BASE, TIME, SPACETIME scenarios). We then applied linear regression

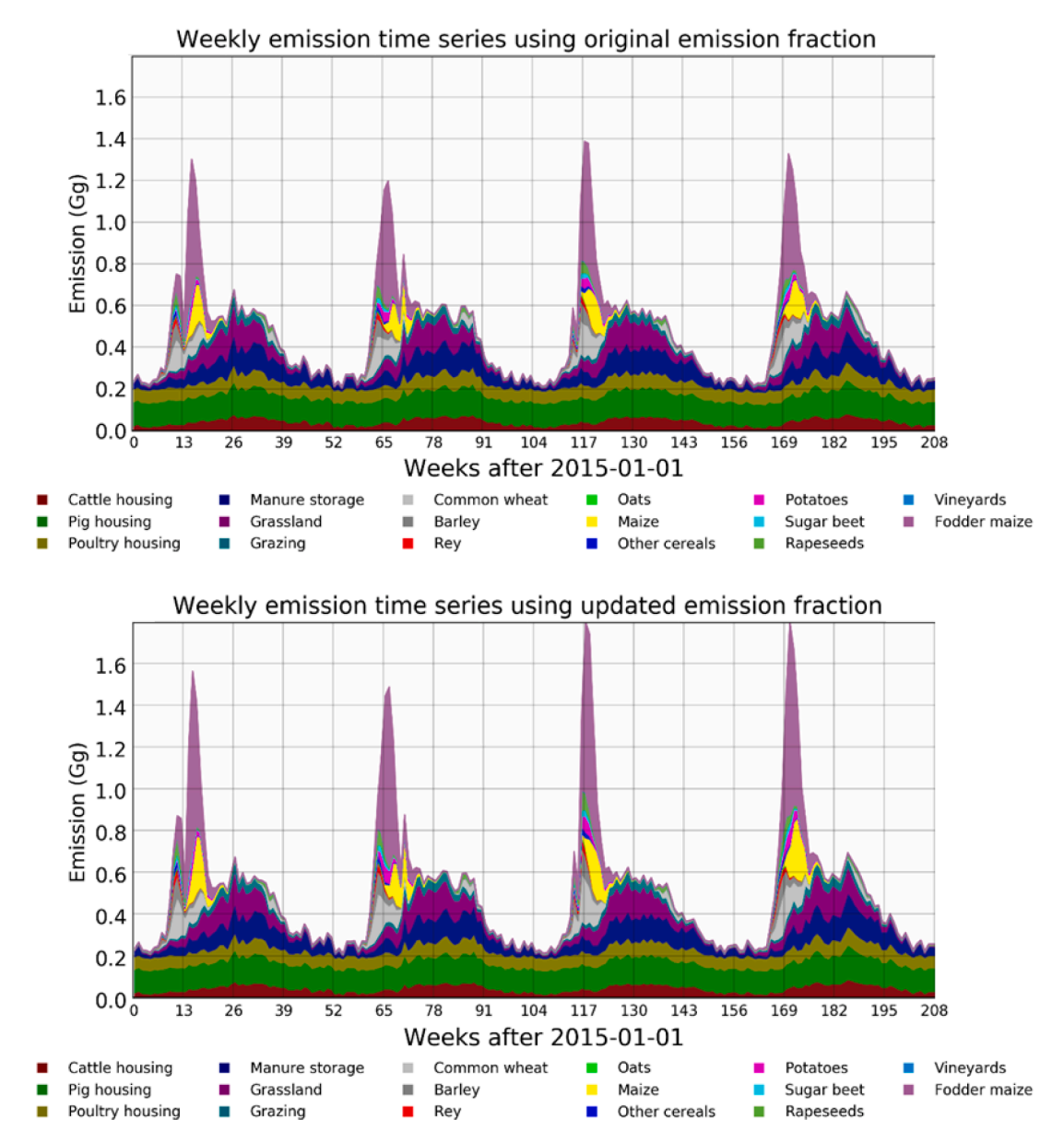
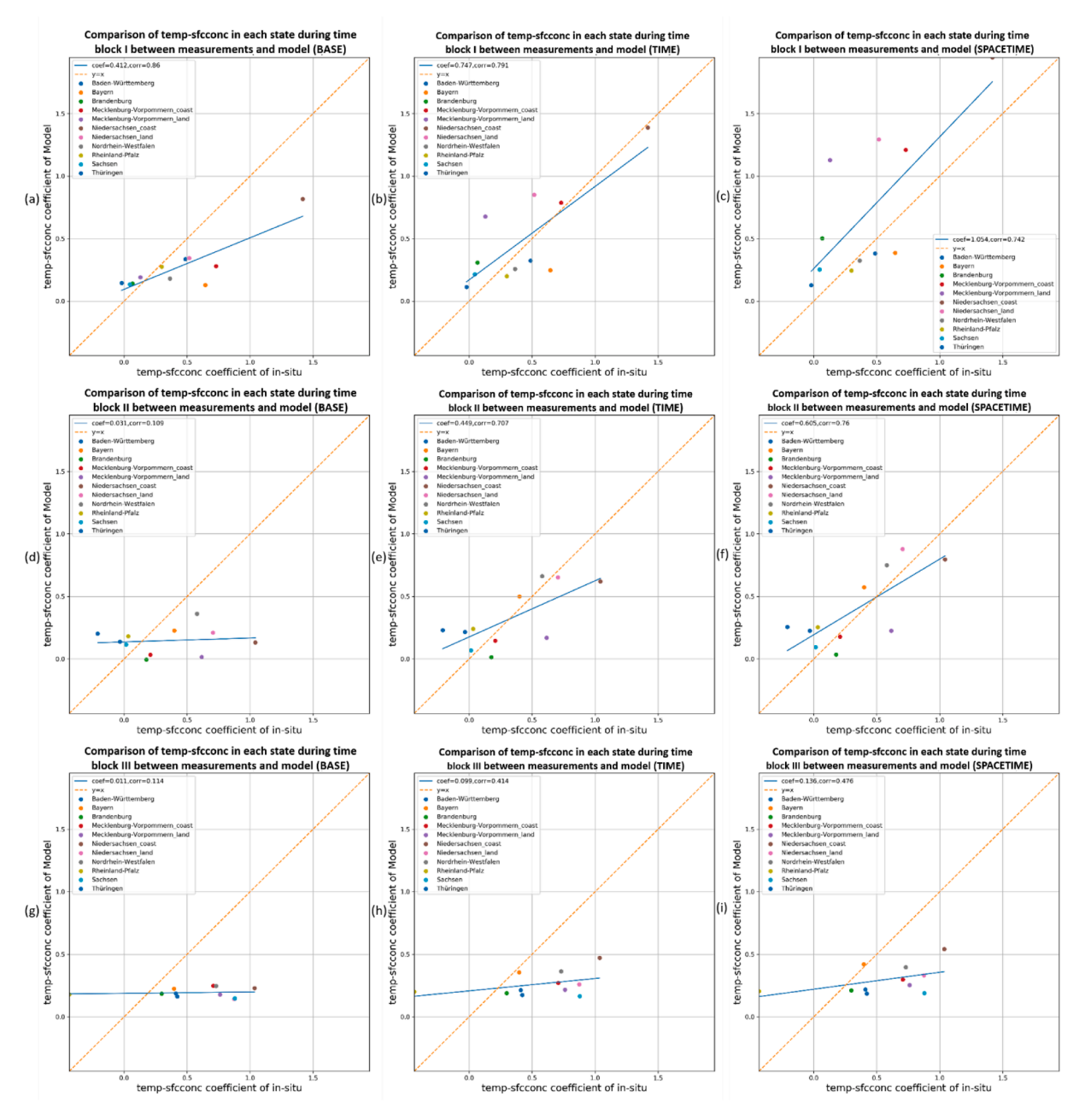


Fig. 3. An example of ammonia emission time series per sector at a selected location in Germany, using INTEGRATOR output scaled with national totals per sector and constant emission fractions (TIME, top) and with updated weather dependents emission fractions (SPACETIME, bottom).

on the slopes, which indicates how well the three simulation runs can represent the changes in surface concentrations brought by temperature in the three periods. It is apparent that from BASE to TIME, there is an improvement in slope reproduction, illustrated by the linear regression line tilting towards v=x. There is further improvement from TIME to SPACETIME, but to a lesser extent. As a result, we assessed the quality of the simulated slopes by calculating the statistics illustrated in Table 5. One can see that for all three time blocks, the comparison between the measured slopes and the BASE results is the worst for almost all indicators except correlation. SPACETIME shows a better linear regression coefficient when compared with measurements than TIME but it performed worse when it comes to other indicators for the time block I, although not to a large extent. It can be observed from Table 5 that the improvement in time blocks I and II, namely in spring, is more obvious than in time block III. To be more specific, all three scenarios do not demonstrate good estimates in summer. This is because the emission in spring is dominated by manure and fertilizer application while emission in summer is more related to animal housing and therefore less sensitive to temperature. To summarize, the improvement from BASE to TIME is larger than that from *TIME* to *SPACETIME* for all three time blocks. It implies that the meteorology-dependent activity time profile is of greater importance when it comes to the reproduction of interannual variability of surface concentrations.

#### 3.3. Simulated and measured total columns in response to temperature

Similar to the comparison of surface concentrations, we also studied the response of averaged total column to temperature during the three time blocks from 2015 to 2018. As an example, the average total column weekly time series of a 1 by 1 degree window in the North Rhine-Westphalia region is shown in Fig. 5. The red vertical lines are the start of spring peaks based on the observations and the gray shows indicate the wintertime. One can see that the CrIS observations differentiate severely from all three scenarios, especially during wintertime, because the satellite instrument measures the thermal signal and becomes less sensitive under colder conditions (with the signal-to-noise ratio decreasing). The autumn of 2015 witnessed an extremely high peak which is not present in all estimates. However, comparing



**Fig. 4.** Comparison of simulated and measured slopes of surface concentrations to temperature in time block I (top; from Day 77 to 137 linked to first spring fertilization), time block II (middle; from Day 147 to 197 linked to second spring fertilization), and time block III (bottom; from Day 207 to 277 representing summer application and housing/storage emissions) for the *BASE* (left), *TIME* (middle) and *SPACETIME* (right) scenarios. The x-axis is the slope (temp-sfcconc coefficient) from the in situ measurements, the y-axis is the slope from the simulations.

Table 5

Quality assessment of the comparison based on simulated and measured slopes of surface concentrations in response to temperature. The scenarios with the best statistics are marked green, the second best is marked yellow.

Time block	Scenario	Fitting Coef.	Correlation	NRMSE (%)	NMAE (%)	EF	IA
1	BASE	0.43	0.86	44	82	-1.48	0.75
	TIME	0.73	0.76	22	41	0.48	0.87
	SPACETIME	1.02	0.71	29	51	0.22	0.76
2	BASE	0.07	0.22	110	224	-13.67	0.28
	TIME	0.52	0.74	36	56	0.07	0.82
	SPACETIME	0.70	0.79	25	47	0.50	0.88
3	BASE	0.01	0.09	511	249	-221.42	0.12
	TIME	0.09	0.40	156	156	-25.73	0.31
	SPACETIME	0.13	0.47	127	128	-15.59	0.38

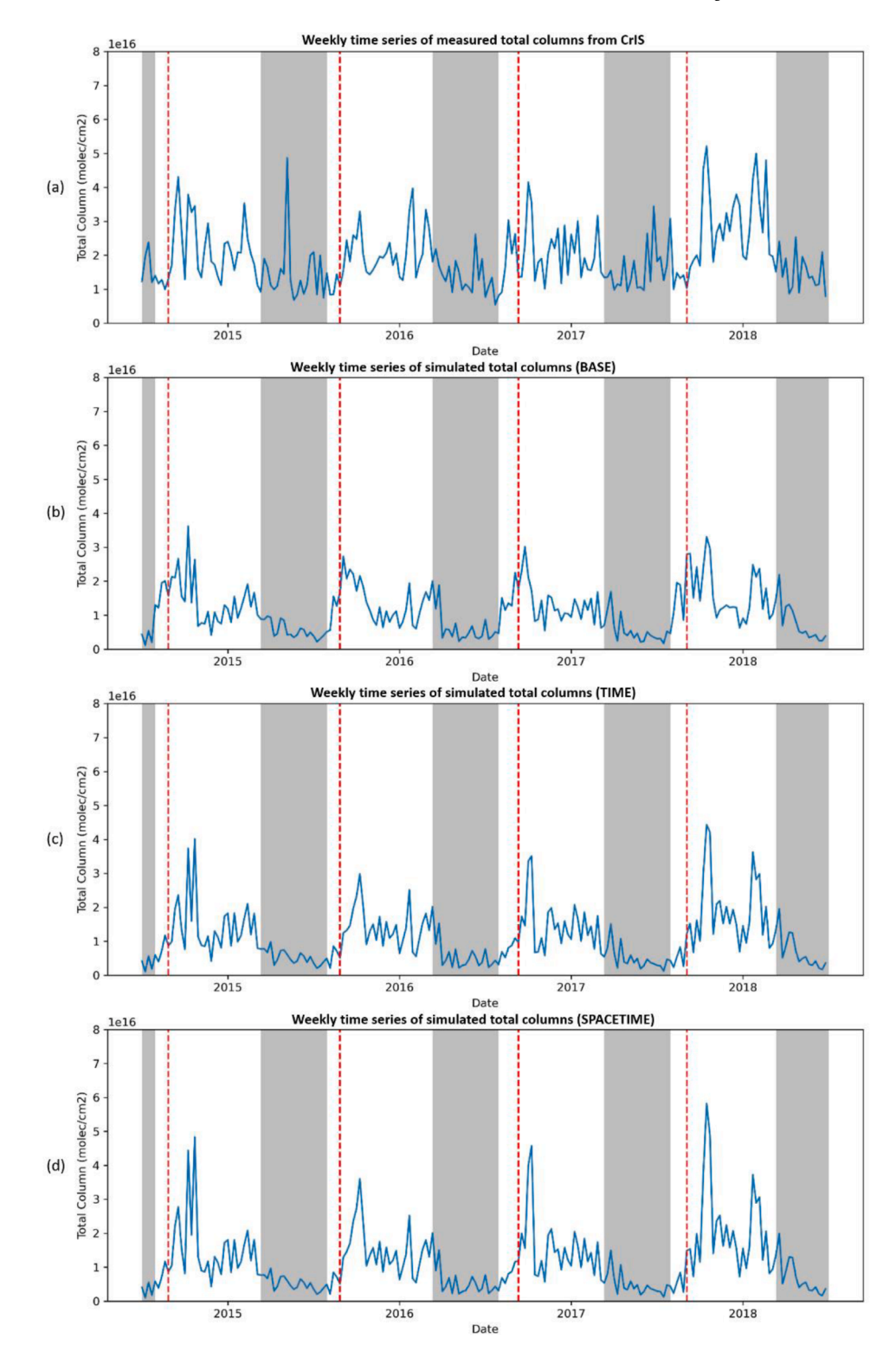
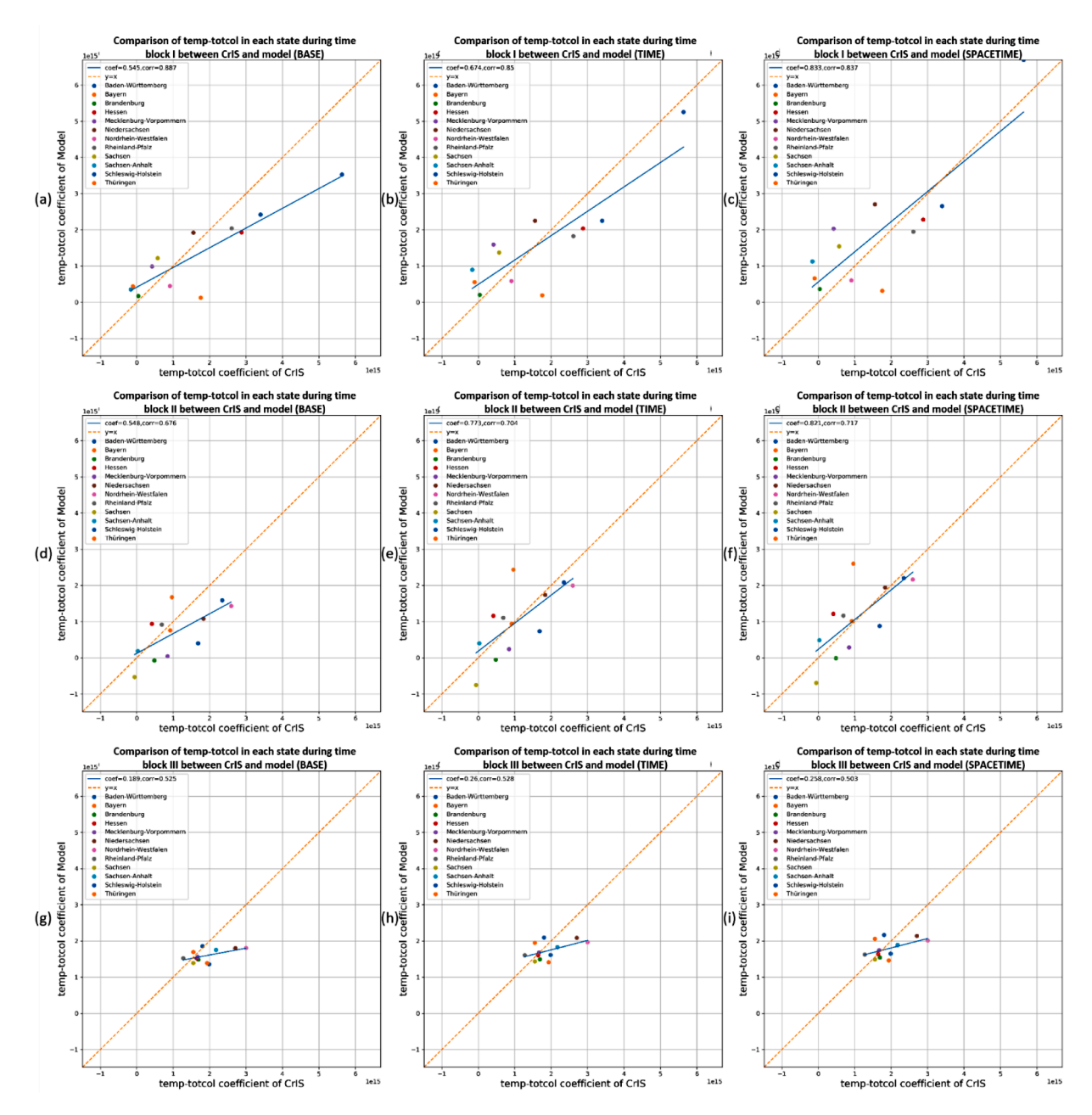


Fig. 5. Weekly time series of total columns between 2015 and 2018 from CrIS observations (a) and simulations of the runs with the scenarios BASE (b), SPACE (c), and SPACETIME (d). The red vertical lines are the start of spring peaks based on the observations and the gray shows indicate the wintertime.

estimates (*TIME* in Fig. 5(c) or *SPACETIME* in Fig. 5(d)) with the satellite measurements (in Fig. 5(a)) indicates that these predicted the peaks more accurately, while Fig. 5(b) exposes the limitation of the static time profile in LOTOS-EUROS.

Fig. 6 shows the comparisons of the slopes (temp-totcol coefficient) of the simulated (from left to right is *BASE, TIME, SPACETIME*) and measured total column in response to temperature in all German states

for the three time blocks (from up to bottom is the time block I, II, III). For the time block I and III, *TIME* and *SPACETIME* both show better predictions of the slope compared to *BASE*. Even though the difference between *TIME* and *SPACETIME* is less noticeable, it is still visible that there is a slight improvement from *TIME* to *SPACETIME*, especially for the time block I. The quality of comparison of trends between total column and temperature is illustrated in *Table 6*. The *SPACETIME* result



**Fig. 6.** Comparison of simulated and measured slopes of total columns to temperature in time block I (top; between Day 77 and 137 linked to first spring fertilization), time block II (middle; between Day 147 and 197 linked to second spring fertilization), and time block III (bottom; between Day 207 and 277 representing summer application and housing/storage emissions) for the *BASE* (left), *TIME* (middle) and *SPACETIME* (right) scenarios. The x-axis is the slope (temp-totcol coefficient) from the satellite measurements, the y-axis is the slope from the simulations.

Table 6
Quality assessment of the comparison of measured and modeled trends of total columns in the three time blocks. The scenarios with the best statistics are marked green, the second best is marked yellow.

Time block	Scenario	Fitting Coef.	Correlation	NRMSE (%)	NMAE (%)	EF	IA
1	BASE	0.54	0.89	28	61	0.13	0.87
	TIME	0.67	0.85	17	50	0.55	0.90
	SPACETIME	0.83	0.84	15	48	0.64	0.91
2	BASE	0.55	0.68	33	90	-0.14	0.76
	TIME	0.77	0.70	21	56	0.45	0.83
	SPACETIME	0.82	0.72	21	50	0.49	0.84
3	BASE	0.19	0.52	104	25	-8.24	0.46
	TIME	0.26	0.53	65	21	-2.59	0.59
	SPACETIME	0.26	0.50	62	19	-2.12	0.60

has outperformed the other two cases in every statistic. Still, the improvement in time block II and III (warmer season) from *TIME* to *SPACETIME* is not as considerable as the comparison of surface concentrations. We can safely conclude that for the springtime, there is an improvement in reproducing total column slopes from *BASE* to *TIME*, while SPACETIME improves further, but to a smaller extent.

#### 4. Discussion and conclusion

This study is based on the previous work of Ge et al. (2020) and included the neglected parameter (meteorology, slurry application techniques and incorporation time, manure properties) in emission fractions estimates. The spatially explicit emission database is aimed to improve the spatial distribution and interannual variability of ammonia emission. We can see a clear improvement in the results but there still exist some uncertainties, which are interpreted and described as follows.

#### 4.1. Comparison of annual emission totals and time series

In general, the update of the emission fractions used in INTEGRATOR for housing and manure storage and slurry manure application resulted in a closer agreement between calculated and official reported emissions (except for the year 2018). Still, for some categories differences were substantial. Cattle and pig management (animal housing and manure storage) contributed to around -45 (-30%) and 30 Gg (33%) difference in annual emission, respectively. Since we scaled the animal number distribution input of INTEGRATOR to match the average state sums of the multi-year official data (which does not vary as strongly as the emissions), the difference should not come from animal numbers of cattle and pigs. Therefore, a likely reason is the different methods to estimate excretion from animal numbers. For example, in INTEGRATOR, it was obtained by multiplying animal numbers with excretion rate which stands for the ratio between the total N excreted and the number of animals (kg N per animal) for each animal type. The coefficients of the INTEGRATOR model come from scaling the GAINS model (Asman et al., 2011), which was submitted by national experts (Klimont and Brink, 2004). The official German excretions, however, were derived using an N-balanced approach (Haenel et al., 2014). In the case of dairy cattle, excretion was calculated by extracting the amount of N retained in weight gained, exported with milk, and in conception products from the amount of N taken in with feed (Haenel et al., 2020). This can explain the underestimation in cattle management emissions reported in this study; a similar explanation can be applied to pig and poultry management.

To further improve the excretion rates, N excretion rates at the regional level can be introduced in INTEGRATOR. For example, Velthof (2014) included the impact of the Nitrates Directive on gaseous N emission in calculating N excretion rates from dairy cattle (in kg per dairy cow per NUTS-2 region). They found out that the N excretion rate is generally higher in the north (115 – 135 kg N per cow) than in the south of Germany (larger than 95 – 115 kg N per cow), with the highest rates in Detmold and Amsberg. In addition, Velthof (2014) showed that N input to grassland (kg N per ha per year) has an impact on N excretion rate (kg N per cow per year). Under the assumption of a total feed requirement of 7000 kg dry matter per cow, the N excretion rate increases almost linearly when N input on grassland increases and the slope rises along with the percentage of grazed grass in the 7000 kg dry matter feed.

In INTEGRATOR, the excretion of animals in housing systems and of grazing animals in pastures is separated, based on data for the number of grazing days at the country level. For the German inventory, N excretions were split into shares for the house, the milking area, and grazing. The division contributed to both the deviation in cattle management emission and grazing emission. Instead of being a country-dependent constant, the division should be more variable as the grazing systems applied and the duration of daytime grazing together determine the

amounts of excretion in animal housing during grazing seasons for dairy cows (van Bruggen et al., 2012). For instance, van Bruggen et al. (2010) assumed that for the Netherlands, excretion amounts in animal housing for day and night grazing and daytime grazing is proportional to the number of barn hours. van Bruggen et al. (2012) categorized grazing systems into unlimited grazing, limited grazing, or full-time housing and presented the percentage of N excretion within housing systems for each grazing system applied. A better survey on the distribution of various grazing systems is needed to derive more accurate estimates of emissions from housing and storage systems at the regional level.

Regarding the trend of manure application emissions, the official data showed a gradual decline over the years, while the updated model output implied a rise between 2016 and 2018. This is because the German inventory used to obtain emission estimates accounts for changes in animal numbers but not for meteorology between years, while our simulations included the impact of meteorology but not animal numbers as we used a 4-year average of the reported values. In addition, uncertainties in the predicted emission fractions affect the simulated emissions. First of all, in many cases, predictions will be based on only limited predictor variables, undoubtedly resulting in inaccurate predictions among locations or even at a single location on different dates (e.g., with differences in soil properties including soil pH and soil water content). Missing variables limit the utility of the ALFAM2 model because, in this case, the ALFAM2 results would be less variable than reality as information on additional driving variables is not available. For example, slurry and soil pH are essential to simulate the impact of the system pH change on ammonia volatilization. In addition, the measurements used to develop ALFAM2 from the individual institutes are not harmonized and balanced, which indicates that the independence of the abundant observations can lead to possible systematic differences. The neglect of variable confoundment (interactions between variables such as soil moisture and manure dry matter) is likely to contribute to bias or inaccurate effect estimates. Therefore, increasing the variety of measurements and improving harmonization through future emission measurement experiments can help to estimate emission fractions better. In particular, emission measurements from regions not well represented in the database would be of great value. It is also essential to include more variables when recording ammonia emissions. Hafner et al. (2018) made a list of minimum recommendations for variables to be measured and reported to ensure valuable results. Systematic biases affect absolute emissions, but not necessarily relative differences. Thus, predictions of relative effects on emission are more accurate than predictions of absolute emission. Since we focused on interannual variation instead of the absolute emission, ALFAM2 was without a doubt of great significance for this study.

The difference in emission total over the years resulted in the same trends of the time series in terms of the magnitudes of peaks (see Fig. 1), as they used the same activity time profile. This is why the spring of 2018 witnessed the highest peak over the five years in Fig. 1(b) while it was in 2017 in Fig. 1(a). If we look at the sector component of the emission time series, the difference mostly came from spring fertilization on fodder maize because fodder maize dominates the crop type in this area and N excretion allocated here is the highest. For other sectors such as animal housing and manure storage, changes from temperaturebased scaling were not significant, especially for insulated buildings with forced ventilation like pig and poultry housing (Gyldenkærne et al., 2005). However, cattle housing and manure storage are more sensitive to temperature variation within a year than between years because the temperature-based scaling ensured that the average ammonia emission level corresponds to the original INTEGRATOR output. To achieve a more accurate emission fraction for housing and manure storage, it is of great help to have access to detailed hourly ammonia measurements over a long period on an extensive network. Sommer et al. (2019) pointed out that during the measurements, it is important to record the following factors defining the housing categories and affecting emission: (1) the ratio of slatted floor to concrete floor area for pigs, (2) floor

opening area, (3) distribution of excreta within the building, which is affected by the positioning of feeders and drinkers, and behavior of pigs as related to age and temperature, (4) capacity of in-house storage, (5) age of animals, (6) climate, and (7) feeding practice.

## 4.2. Comparison of simulated and measured slopes of surface concentrations with respect to temperature

Regarding surface concentration's response to temperature (tempsfcconc calculated as the slope of linear regression), we included the BASE scenario to investigate to which extent the updated emission fractions or spatially explicit time profiles improved the estimates compared to in situ measurements. When we compared the slopes tempsfcconc, the simulations based on the TIME scenario compared much better with observations than those from the BASE scenario, while the SPACETIME scenario usually outperformed TIME, but to a lesser extent. It implies that using a spatially explicit time allocation (Ge et al., 2020) improves the model's ability to detect ammonia interannual variability (brought by meteorology), while the utilization of weather-dependent emission fractions improves the simulations further. The improvement was bigger in spring than in summer, which may be caused by three reasons. First, the summer ammonia level in the model was usually dominated by animal housing and manure storage, among which only cattle housing is more sensitive to temperature since cattle houses were considered open houses. As a result, the slope temp-sfcconc brought from the slurry application emission fraction is less noticeable. Another reason is that the absolute temperature is higher in summer. Sutton et al. (2013) concluded from the results of various field campaigns that the percentage of N volatilized as ammonia increased exponentially as a function of average temperature. Bleizgys et al. (2013) also found similar correlations from experiment results from a naturally ventilated open cowshed lab, namely, ammonia increased emission gains at higher temperatures. This behavior was also captured by the modeled results from ALFAM2. It means that the calculated emission fractions are more sensitive to uncertainties. Another factor that could affect the quality of the trend comparisons is the separation of the three time blocks. Time block I (from Day 77 to 137) is linked to first spring fertilization), time block II (between Day 147 and 197) is related to second spring fertilization), and time block III (from Day 207 to 277) represents summer application and housing/storage emissions). The separation was derived using visual inspection to distinguish multiple fertilizations. However, as Ge et al. (2020) pointed out, the sowing (fertilization) day of a certain crop varies according to temperature, rainfall, and legislative constraints, with the temperature being the dominant factor. Therefore, when it comes to a relatively larger country like Germany, the separation of time blocks might be more flexible.

## 4.3. Comparison of simulated and measured slopes of total columns with respect to temperature

Regarding simulated slopes of total columns with respect to temperature (temp-totcol), the simulations based on the *TIME* scenario compared much better with observations than those from the BASE scenario for time blocks I and II, but the improvement was much less visible for time block III, as well as from *TIME* to *SPACETIME* was weaker. Therefore, we can come to a similar conclusion that spatially explicit time profiles (Ge et al., 2020) improve the model's ability to detect ammonia interannual variability, while the newly developed emission fractions improve the simulations more, especially for springtime. The improvements in total column slopes are not very apparent in summer, which could be caused by the following reasons. One possible reason is the uncertainties in total column measurement from the CrIS instrument. Even though the higher temperature in summer makes CrIS more sensitive, the uncertainties in summer are also higher.

Another factor is that we defined a threshold before calculating averaged total columns per state to only include the ammonia hot spot during the agriculturally active period. Because 1) there is a minimum detection value of ammonia in CrIS observations and 2) we wanted to exclude background ammonia levels over the non-agricultural area (forest and urban). It should be mentioned that the threshold to exclude background ammonia also has an impact on the overall performance. We also did a sensitivity study on how the threshold can impact the quality of the comparison. When the threshold increased from 0 to approximately  $1 \times 10^{16} molec/cm^2$ , the improvement in calculated total column slope in the SPACETIME scenario went from unclear (random trends) to gradually visible. After  $1 \times 10^{16} molec/cm^2$ , the improvement of SPACETIME declined, especially for time block III. It means that the model performance worsens when selectively focusing on high levels of ammonia in summer, which could be caused by the spatial allocation of emissions from animal housing and manure storage. Emissions from animal houses and manure storage facilities should be seen as point sources, but due to the absence of information on the locations of animal houses, we evenly distributed them all over the NCUs, which smoothens the emission hot spots of animal housing. During the first stage of the threshold increase from 0 to approximately  $1 \times 10^{16} molec/cm^2$ , the background constant ammonia was gradually excluded. The second stage of the threshold increase after  $1 \times 10^{16} molec/cm^2$ , however, exposed the shortcoming of the spatial allocation of housing emissions. Since housing emissions were more spread out instead of point sources, they were excluded as well. This also explains the reduced improvement over summer because housing emissions became more dominant as application emissions in summer dropped compared to spring. Consequently, access to the coordinates of animal houses to attribute emissions to the right locations would be helpful. Ge et al. (2022) confirmed for the Netherlands that the improvement brought about by the detailed information on housing locations is significant. Without housing locations, the emissions from animal houses and manure storage facilities were distributed all over the NCU, which resulted in smoothened spatial

We also compared the weekly total column time series of a selected 1 by 1 degree window from CrIS observations with the modeled results from the three scenarios (Fig. 5). When it comes to spring peaks, the BASE scenario always overestimated the total columns at the beginning of the year because the fixed time profile used does not account for the actual practice of fertilization which is affected by temperature and resembles the spring peak earlier than reality. On the contrary, for both the TIME and SPACETIME cases which used the same time profile, the spring peaks synchronized with CrIS measurements, which also validates the time profile algorithm of Ge et al. (2020). In addition, the comparison in winter seemed quite poor. This is because satellite observations measure in the infrared portion of the radiation source. When the thermal signal is decreased under colder conditions (such as in winter), the overall signal-to-noise ratio (SNR) and sensitivity will reduce (Dammers et al., 2019). Furthermore, the number of observations that pass the quality criteria is much lower than in spring and summer. Therefore, we focused on the period between 1 March and 30 September. Shephard et al. (2020) proposed to average CrIS observations over longer periods (e.g. monthly, seasonal, and annual) instead of

The comparison of the ammonia total column implies that better satellite data is of great importance, which requires higher spatial resolution, higher sensitivity and shorter revisit time. The revisit time can be improved by assimilating various data sources such as IASI, but data harmonization would be needed. For now, satellite measurements are valuable for the validation of ammonia budgets over a larger region or a long period. It is however not yet sufficient for point sources or grid cells of limited size less than the measurements' spatial resolution.

#### 4.4. Conclusions and outlook

In this study, we presented an ammonia emission inventory using

weather (air temperature, wind speed, and rainfall rate) dependent emission fractions for slurry application to crops (obtained with ALFAM2), and temperature-dependent emission fractions for animal housing and manure storage, aiming to improve the model's ability to reproduce interannual variation observed in satellite observations and in situ measurements. The emission fractions for slurry application also accounted for differences in dry matter content and pH of the slurry and slurry application method. The newly modeled annual emission totals (and manure application emissions) were closer to the officially reported values (except for 2018), but deviations in some categories (cattle and pig housing/storage) remained relatively large. For emissions from animal housing and manure storage, the temperature-based scaling method affects the spatial distribution and temporal distribution within a year and between years, rather than the absolute magnitude. Compared to a national generic time allocation of emission within the year, a spatially explicit time profile already largely improved the ability to reproduce interannual ammonia surface concentrations and total columns. The updated weather-dependent emission fractions further improved the comparison of simulated and measured surface concentrations and total columns. This study showed that modeling the variability of ammonia emissions is a crucial step to improve the performance (the comparison of predicted and observed variability in ammonia concentration levels) of chemistry transport models.

To further develop the modeling of ammonia emissions from agriculture, priorities should focus on improving both the spatial and temporal distribution of emission estimates, as well as the retrievals of ground-based surface concentrations and satellite-derived total columns for validation. Several aspects can improve ammonia emission modeling. First of all, the spatial details of basic input data for the model can be refined, including livestock and crop distributions, animal housing locations, fertilizer use, application techniques and incorporation times, and timing of fertilization. Secondly, the ammonia emission functions (emission fractions and temporalization) should be further developed by better accounting for impacts of site conditions, including crop type, climate, and soil properties, which are regionally available. Last but not least, data affecting the N manure input, and thus the ammonia emission, can also be ameliorated, including N excretion rates and the division of N excretion over grazing and housing. In situ measurements offer great possibilities for the validation of temporal variations while satellite-derived observations can be used to validate the spatial variation in large-scale estimates of ammonia emissions. However, most ground stations in Western Europe offer concentrations at the monthly resolution, which is not detailed enough to validate the timing of emission from manure and fertilizer application. The progressing development of satellite remote sensing nowadays provides great opportunities for better constraining ammonia emissions in space and time. Since approximately 2018, CrIS and IASI satellite observations, combined with relevant emission inventory, have been widely to calculate NH3 emission fluxes and identify ammonia emission hotspots at the global scale (Clarisse et al., 2019; Dammers et al., 2019; Evangeliou et al., 2021; Luo et al., 2022; Van Damme et al., 2018). At the regional scale, it is also feasible to make use of satellite data, combined with high-resolution emission inventories, to reduce the uncertainties in ammonia emission and deposition in space and time. For instance, we can take advantage of the averaging kernels and error covariance matrix provided in the CrIS retrieved product to provide top-down constraints on the ammonia emissions (Cao et al., 2020; Shephard et al., 2020). Examples of use at the regional scale are still quite limited with notable examples of their application in the UK (Marais et al., 2021), the US (Chen et al., 2021), and China (Liu et al., 2022). To improve ammonia total columns observed by CrIS, we can refine the retrievals over elevated concentration values on high elevations wintertime conditions and enhance the a-priori profiles and constraints used in the retrieval (Shephard et al., 2020).

#### **Declaration of competing interest**

The authors declare that they have no known competing financial interests or personal relationships that could have appeared to influence the work reported in this paper.

#### Data availability

Data will be made available on request.

#### Acknowledgments

We thankfully acknowledge the Nederlandse Organisatie voor Wetenschappelijk Onderzoek (NWO), which financially supported this research as part of the AMARETTO (Air pollutant emissions from agriculture optimized by Earth observations) project (projectnr. ALW-GO/16-02). We also like to thank Dr. Sasha Hafner and his team for their work on the ALFAM2 model.

#### Data availability

The updated ammonia emission fractions and annual ammonia emission distribution are available by request.

#### Code availability

LOTOS-EUROS is available for download under license at https://lotos-euros.tno.nl/.

#### Author contribution

Xinrui Ge designed and programmed the processing chain, performed the simulations, and analyzed the results for discussion and conclusion. Martijn Schaap provided his expertise in atmospheric modeling and sciences and helped with the interpretation of the results. Enrico Dammers offered his knowledge on the satellite retrievals of ammonia total columns. Mark Shephard shared his dataset of ammonia total columns. Wim de Vries is the promotor of the project and he offered his knowledge regarding nitrogen use on crops and ammonia emission from agriculture.

#### Supplementary materials

Supplementary material associated with this article can be found, in the online version, at doi:10.1016/j.agrformet.2023.109432.

#### References

- Amann, M., Klimont, Z., Wagner, F., 2013. Regional and global emissions of air pollutants: recent trends and future scenarios. https://doi.org/10.1146/annurevenviron-052912-173303 38, 31–55. 10.1146/ANNUREV-ENVIRON-052912-1 73303.
- Asman, W.A.H., Klimont, Z., Winiwarter, W., 2011. A simplified model of nitrogen flows from manure management. IR-11-030, IIASA, Laxenburg, Austria.
- Backes, A., Aulinger, A., Bieser, J., Matthias, V., Quante, M., 2016. Ammonia emissions in Europe, part I: development of a dynamical ammonia emission inventory. Atmos. Environ. 131, 55–66. https://doi.org/10.1016/j.atmosenv.2016.01.041.
- Bleizgys, R., Bagdonienė, I., Baležentienė, L., 2013. Reduction of the livestock ammonia emission under the changing temperature during the initial manure nitrogen biomineralization. Sci. World J., 825437 https://doi.org/10.1155/2013/825437, 2013.
- Cao, H., Henze, D.K., Shephard, M.W., Dammers, E., Cady-Pereira, K., Alvarado, M., Lonsdale, C., Luo, G., Yu, F., Zhu, L., Danielson, C.G., Edgerton, E.S., 2020. Inverse modeling of NH3 sources using CrIS remote sensing measurements. Environ. Res. Lett. 15, 104082 https://doi.org/10.1088/1748-9326/abb5cc.
- Cao, H., Henze, D.K., Zhu, L., Shephard, M.W., Cady-Pereira, K., Dammers, E., Sitwell, M., Heath, N., Lonsdale, C., Bash, J.O., Miyazaki, K., Flechard, C., Fauvel, Y., Kruit, R.W., Feigenspan, S., Brümmer, C., Schrader, F., Twigg, M.M., Leeson, S., Tang, Y.S., Stephens, A.C.M., Braban, C., Vincent, K., Meier, M., Seitler, E., Geels, C., Ellermann, T., Sanocka, A., Capps, S.L., 2022. 4D-var inversion of European NH3

- emissions using CrIS NH3 measurements and GEOS-Chem adjoint with Bi-directional and uni-directional flux schemes. J. Geophys. Res. Atmos. 127, e2021JD035687. https://doi.org/10.1029/2021JD035687.
- Cellier, P., Durand, P., Hutchings, N., Dragosits, U., Theobald, M., Drouet, J.-L., Oenema, O., Bleeker, A., Breuer, L., Dalgaard, T., Duretz, S., Kros, J., Loubet, B., Olesen, J.E., Merot, P., Viaud, V., de Vries, W., Sutton, M.A., 2011. Nitrogen flows and fate in rural landscapes. Eds.. In: Sutton, M.A., Howard, C.M., Erisman, J.W., Billen, G., Bleeker, A., Grennfelt, P., van Grinsven, H., Grizzetti, B. (Eds.), The European Nitrogen Assessment: Sources, Effects and Policy Perspectives. Cambridge University Press, Cambridge, pp. 229–248.
- Chantigny, M.H., Rochette, P., Angers, D.A., Massé, D., Côté, D., 2004. Ammonia volatilization and selected soil characteristics following application of anaerobically digested pig slurry. Soil Sci. Soc. Am. J. 68, 306–312. https://doi.org/10.2136/SSSAJ2004.3060.
- Chen, Y., Shen, H., Kaiser, J., Hu, Y., Capps, S.L., Zhao, S., Hakami, A., Shih, J.-S., Pavur, G.K., Turner, M.D., Henze, D.K., Resler, J., Nenes, A., Napelenok, S.L., Bash, J.O., Fahey, K.M., Carmichael, G.R., Chai, T., Clarisse, L., Coheur, P.-F., Van Damme, M., Russell, A.G., 2021. High-resolution hybrid inversion of IASI ammonia columns to constrain US ammonia emissions using the CMAQ adjoint model. Atmos. Chem. Phys. 21, 2067–2082. https://doi.org/10.5194/acp-21-2067-2021.
- Clarisse, L., Clerbaux, C., Dentener, F., Hurtmans, D., Coheur, P.F., 2009. Global ammonia distribution derived from infrared satellite observations. Nat. Geosci. 2, 479–483. https://doi.org/10.1038/ngeo551.
- Clarisse, L., Van Damme, M., Clerbaux, C., Coheur, P.-F., 2019. Tracking down global \chem{NH\_3} point sources with wind-adjusted superresolution. Atmos. Meas. Tech. 12, 5457–5473. https://doi.org/10.5194/amt-12-5457-2019.
- Congreves, K.A., Grant, B.B., Dutta, B., Smith, W.N., Chantigny, M.H., Rochette, P., Desjardins, R.L., 2016. Predicting ammonia volatilization after field application of swine slurry: DNDC model development. Agric. Ecosyst. Environ. 219, 179–189. https://doi.org/10.1016/j.agee.2015.10.028.
- Cuddington, K., Fortin, M.-J., Gerber, L.R., Hastings, A., Liebhold, A., O'Connor, M., Ray, C., 2013. Process-based models are required to manage ecological systems in a changing world. Ecosphere 4, art20. 10.1890/ES12-00178.1.
- Dammers, E., McLinden, C.A., Griffin, D., Shephard, M.W., Van Der Graaf, S., Lutsch, E., Schaap, M., Gainairu-Matz, Y., Fioletov, V., Van Damme, M., Whitburn, S., Clarisse, L., Cady-Pereira, K., Clerbaux, C., Francois Coheur, P., Erisman, J.W., 2019. NH3 emissions from large point sources derived from CrIS and IASI satellite observations. Atmos. Chem. Phys. 19, 12261–12293. https://doi.org/10.5194/ACP-19-12261-2019
- Dämmgen, U., Hutchings, N.J., 2008. Emissions of gaseous nitrogen species from manure management: a new approach. Environ. Pollut. 154, 488–497. https://doi.org/ 10.1016/J.ENVPOL.2007.03.017.
- de Vries, W., 2021. Impacts of nitrogen emissions on ecosystems and human health: a mini review. Curr. Opin. Environ. Sci. Heal. 21, 100249 https://doi.org/10.1016/J. COESH.2021.100249.
- de Vries, W., Kros, J., Dolman, M.A., Vellinga, T.V., de Boer, H.C., Gerritsen, A.L., Sonneveld, M.P.W., Bouma, J., 2015. Environmental impacts of innovative dairy farming systems aiming at improved internal nutrient cycling: a multi-scale assessment. Sci. Total Environ. 536, 432–442. https://doi.org/10.1016/j. scitoteny. 2015.07.079
- De Vries, W., Leip, A., Reinds, G.J., Kros, J., Lesschen, J.P., Bouwman, A.F., 2011. Comparison of land nitrogen budgets for European agriculture by various modeling approaches. Environ. Pollut. 159, 3254–3268. https://doi.org/10.1016/j. envpol.2011.03.038.
- De Vries, W., Schulte-Uebbing, L., Kros, J., 2020. Assessment of Spatially Explicit Actual, Required and Critical Nitrogen Inputs in EU-27 Agriculture (in press). Wageningen.
- Dominguez-Rodriguez, A., Baez-Ferrer, N., Rodríguez, S., Avanzas, P., Abreu-Gonzalez, P., Terradellas, E., Cuevas, E., Basart, S., Werner, E., 2020. Saharan dust events in the Dust Belt -Canary Islands- and the observed association with in-hospital mortality of patients with heart failure. J. Clin. Med. 9, 376. https://doi.org/10.3390/JCM9020376, 2020VolPage 376 9.
- Erisman, J.W., 2021. How ammonia feeds and pollutes the world. Science 374 (80), 685–686. https://doi.org/10.1126/SCIENCE.ABM3492.
- European Environment Agency, 2019. NEC Directive reporting status 2019.
- Evangeliou, N., Balkanski, Y., Eckhardt, S., Cozic, A., Van Damme, M., Coheur, P.-F., Clarisse, L., Shephard, M.W., Cady-Pereira, K.E., Hauglustaine, D., 2021. 10-year satellite-constrained fluxes of ammonia improve performance of chemistry transport models. Atmos. Chem. Phys. 21, 4431–4451. https://doi.org/10.5194/acp-21-4431-2021.
- Forsius, M., Posch, M., Holmberg, M., Vuorenmaa, J., Kleemola, S., Augustaitis, A., Beudert, B., Bochenek, W., Clarke, N., de Wit, H.A., Dirnböck, T., Frey, J., Grandin, U., Hakola, H., Kobler, J., Krám, P., Lindroos, A.J., Löfgren, S., Pecka, T., Rönnback, P., Skotak, K., Szpikowski, J., Ukonmaanaho, L., Valinia, S., Váňa, M., 2021. Assessing critical load exceedances and ecosystem impacts of anthropogenic nitrogen and sulphur deposition at unmanaged forested catchments in Europe. Sci. Total Environ. 753, 141791 https://doi.org/10.1016/J.SCITOTENV.2020.141791.
- Gac, A., Béline, F., Bioteau, T., Maguet, K., 2007. A French inventory of gaseous emissions (CH4, N2O, NH3) from livestock manure management using a mass-flow approach. Livest. Sci. https://doi.org/10.1016/j.livsci.2007.09.006.
- Ge, X., Schaap, M., de Vries, W., 2022. Improving spatial and temporal variation of ammonia emissions for the Netherlands using livestock housing information and a sentinel-2-derived Crop Map. SSRN Electron. J. https://doi.org/10.2139/ SSRN 4028270
- Ge, X., Schaap, M., Kranenburg, R., Segers, A., Reinds, G.J., Kros, H., de Vries, W., 2020. Modeling atmospheric ammonia using agricultural emissions with improved spatial

- variability and temporal dynamics. Atmos. Chem. Phys. 20, 16055-16087. https://doi.org/10.5194/acp-20-16055-2020.
- Génermont, S., Cellier, P., 1997. A mechanistic model for estimating ammonia volatilization from slurry applied to bare soil. Agric. For. Meteorol. 88, 145–167. https://doi.org/10.1016/S0168-1923(97)00044-0.
- Gericke, D., Bornemann, L., Kage, H., Pacholski, A., 2012. Modelling ammonia losses after field application of biogas slurry in energy crop rotations. Water, Air, Soil Pollut 223, 29–47. https://doi.org/10.1007/s11270-011-0835-4.
- Giannadaki, D., Giannakis, E., Pozzer, A., Lelieveld, J., 2018. Estimating health and economic benefits of reductions in air pollution from agriculture. Sci. Total Environ. 1304–1316. https://doi.org/10.1016/j.scitotenv.2017.12.064, 622–623.
- Gyldenkærne, S., Skjøth, C.A., Hertel, O., Ellermann, T., 2005. A dynamical ammonia emission parameterization for use in air pollution models. J. Geophys. Res. Atmos. 110, 1–14. https://doi.org/10.1029/2004JD005459.
- Haenel, H.-D., Rösemann, C., Dämmgen, U., Döring, U., Wulf, S., Eurich-Menden, B., Freibauer, A., Döhler, H., Schreiner, C., Osterburg, B., Fuß, R., 2020. Calculations of gaseous and particulate emissions from German agriculture 1990 - 2018: Input data and emission results. 10.3220/DATA20200312140923.
- Haenel, H.-D., Rösemann, C., Dämmgen, U., Poddey, E., Freibauer, A., Wulf, S., Eurich-Menden, B., Döhler, H., Schreiner, C., Bauer, B., Osterburg, B., 2014. Calculations of gaseous and particulate emissions from German agriculture 1990 2012: Report on methods and data (RMD) Submission 2014, Berechnung von gas- und partikelförmigen Emissionen aus der deutschen Landwirtschaft 1990 2012: Report zu Methoden u. Johann Heinrich von Thünen-Institut, Braunschweig. https://doi.org/10.3220/REP\_17\_2014.
- Hafner, S.D., Pacholski, A., Bittman, S., Burchill, W., Bussink, W., Chantigny, M., Carozzi, M., Génermont, S., Häni, C., Hansen, M.N., Huijsmans, J., Hunt, D., Kupper, T., Lanigan, G., Loubet, B., Misselbrook, T., Meisinger, J.J., Neftel, A., Nyord, T., Pedersen, S.V., Sintermann, J., Thompson, R.B., Vermeulen, B., Vestergaard, A.V., Voylokov, P., Williams, J.R., Sommer, S.G., 2018. The ALFAM2 database on ammonia emission from field-applied manure: description and illustrative analysis. Agric. For. Meteorol. 258, 66–79. https://doi.org/10.1016/J. AGREORMET.2017.11.027.
- Hafner, S.D., Pacholski, A., Bittman, S., Carozzi, M., Chantigny, M., Génermont, S., Häni, C., Hansen, M.N., Huijsmans, J., Kupper, T., Misselbrook, T., Neftel, A., Nyord, T., Sommer, S.G., 2019. A flexible semi-empirical model for estimating ammonia volatilization from field-applied slurry. Atmos. Environ. 199, 474–484. https://doi.org/10.1016/j.atmosenv.2018.11.034.
- Hellsten, S., Dragosits, U., Place, C.J., Vieno, M., Dore, A.J., Misselbrook, T.H., Tang, Y. S., Sutton, M.A., 2008. Modelling the spatial distribution of ammonia emissions in the UK. Environ. Pollut. 154, 370–379. https://doi.org/10.1016/J. ENVPOL.2008.02.017.
- Hendriks, C., Kranenburg, R., Kuenen, J., van Gijlswijk, R., Wichink Kruit, R., Segers, A., Denier van der Gon, H., Schaap, M., 2013. The origin of ambient particulate matter concentrations in the Netherlands. Atmos. Environ. 69, 289–303. https://doi.org/ 10.1016/J.ATMOSENV.2012.12.017.
- Hendriks, C., Kranenburg, R., Kuenen, J.J.P., Van den Bril, B., Verguts, V., Schaap, M., 2016. Ammonia emission time profiles based on manure transport data improve ammonia modelling across north western Europe. Atmos. Environ. 131, 83–96. https://doi.org/10.1016/j.atmosenv.2016.01.043.
- Hettelingh, J., Posch, M., Slootweg, J., 2017. European critical loads: database, biodiversity and ecosystems at risk: CCE Final Report 2017. 10.21945/RIVM-2017-
- Huijsmans, J.F.M., 2003. Manure Application and Ammonia Volatilization. Institute of Agricultural and Environmental Engineering (IMAG).
- Huijsmans, J.F.M., Vermeulen, G.D., Hol, J.M.G., Goedhart, P.W., 2018. A model for estimating seasonal trends of ammonia emission from cattle manure applied to grassland in the Netherlands. Atmos. Environ. 173, 231–238. https://doi.org/ 10.1016/J.ATMOSENV.2017.10.050.
- Hutchings, N.J., Reinds, G.J., Leip, A., Wattenbach, M., Bienkowski, J.F., Dalgaard, T., Dragosits, U., Drouet, J.L., Durand, P., Maury, O., De Vries, W., 2012. A model for simulating the timelines of field operations at a European scale for use in complex dynamic models. Biogeosciences 9, 4487–4496. https://doi.org/10.5194/bg-9-4487-2012
- Hutchings, N.J., Sommer, S.G., Andersen, J.M., Asman, W.A.H., 2001. A detailed ammonia emission inventory for Denmark. Atmos. Environ. 35, 1959–1968. https:// doi.org/10.1016/S1352-2310(00)00542-2.
- Jiang, J., Stevenson, D.S., Uwizeye, A., Tempio, G., Sutton, M.A., 2021. A climate-dependent global model of ammonia emissions from chicken farming. Biogeosciences 18, 135–158. https://doi.org/10.5194/bg-18-135-2021.
- Jin, J., Segers, A., Lin, H.X., Henzing, B., Wang, X., Heemink, A., Liao, H., 2021. Position correction in dust storm forecasting using LOTOS-EUROS v2.1: Grid-distorted data assimilation v1.0. Geosci. Model Dev 14, 5607–5622. https://doi.org/10.5194/ GMD-14-5607-2021.
- Joubin, M.L., 2018. Animal slurry acidification: effects of slurry characteristics, use of different acids, slurry pH buffering: Student work.
- Klimont, Z., Brink, C., 2004. Modeling of emissions of air pollutants and greenhouse gases from agricultural sources in Europe. IR-04-048, IIASA, Laxenburg, Austria.
- Kros, J., Heuvelink, G.B.M., Reinds, G.J., Lesschen, J.P., Ioannidi, V., De Vries, W., 2012. Uncertainties in model predictions of nitrogen fluxes from agro-ecosystems in Europe. Biogeosciences 9, 4573–4588. https://doi.org/10.5194/bg-9-4573-2012.
- Kros, J., Hutchings, N.J., Kristensen, I.T.I.S., Kristensen, I.T.I.S., Børgesen, C.D., Voogd, J. C., Dalgaard, T., de Vries, W., 2018. A comparison of disaggregated nitrogen budgets for Danish agriculture using Europe-wide and national approaches. Sci. Total Environ. 643, 890–901. https://doi.org/10.1016/j.scitotenv.2018.06.267.

- Leip, A., Billen, G., Garnier, J., Grizzetti, B., Lassaletta, L., Reis, S., Simpson, D., Sutton, M.A., De Vries, W., Weiss, F., Westhoek, H., 2015. Impacts of European livestock production: nitrogen, sulphur, phosphorus and greenhouse gas emissions, land-use, water eutrophication and biodiversity. Environ. Res. Lett. 10, 115004 https://doi.org/10.1088/1748-9326/10/11/115004.
- Li, C., Salas, W., Zhang, R., Krauter, C., Rotz, A., Mitloehner, F., 2012. Manure-DNDC: A biogeochemical process model for quantifying greenhouse gas and ammonia emissions from livestock manure systems. Nutr. Cycl. Agroecosyst. 93, 163–200. https://doi.org/10.1007/S10705-012-9507-Z/TABLES/10.
- Li, Y., Schwandner, F.M., Sewell, H.J., Zivkovich, A., Tigges, M., Raja, S., Holcomb, S., Molenar, J.V, Sherman, L., Archuleta, C., Lee, T., Collett, J.L., 2014. Observations of ammonia, nitric acid, and fine particles in a rural gas production region. Atmos. Environ. 83, 80–89. https://doi.org/10.1016/j.atmosenv.2013.10.007.
- Liu, P., Ding, J., Liu, L., Xu, W., Liu, X., 2022. Estimation of surface ammonia concentrations and emissions in China from the polar-orbiting infrared atmospheric sounding interferometer and the FY-4A geostationary interferometric infrared sounder. Atmos. Chem. Phys. 22, 9099–9110. https://doi.org/10.5194/acp-22-9094-2022
- Luo, Z., Zhang, Y., Chen, W., Van Damme, M., Coheur, P.-F., Clarisse, L., 2022. Estimating global ammonia (NH\$\_{3}\$) emissions based on IASI observations from 2008 to 2018. Atmos. Chem. Phys. 22, 10375–10388. https://doi.org/10.5194/acp-22-10375-2022.
- Manders, A.M.M., Builtjes, P.J.H., Curier, L., Gon, H.A.C.D., Vander Hendriks, C., Jonkers, S., Kranenburg, R., Kuenen, J.J.P., Segers, A.J., Timmermans, R.M.A., Visschedijk, A.J.H., Kruit, R.J.W., Pul, W.A.J.V., Sauter, F.J., Van Der Swaluw, E., Swart, D.P.J., Douros, J., Eskes, H., Van Meijgaard, E., Van Ulft, B., Van Velthoven, P., Banzhaf, S., Mues, A.C., Stern, R., Fu, G., Lu, S., Heemink, A., Van Velzen, N., Schaap, M., 2017. Curriculum vitae of the LOTOS-EUROS (v2.0) chemistry transport model. Geosci. Model Dev. https://doi.org/10.5194/gmd-10-4145-2017
- Marais, E.A., Pandey, A.K., Van Damme, M., Clarisse, L., Coheur, P.-F., Shephard, M.W., Cady-Pereira, K.E., Misselbrook, T., Zhu, L., Luo, G., Yu, F., 2021. UK ammonia emissions estimated with satellite observations and GEOS-Chem. J. Geophys. Res. Atmos. 126 https://doi.org/10.1029/2021JD035237 e2021JD035237.
- Marécal, V., Peuch, V.H., Andersson, C., Andersson, S., Arteta, J., Beekmann, M., Benedictow, A., Bergström, R., Bessagnet, B., Cansado, A., Chéroux, F., Colette, A., Coman, A., Curier, R.L., Van Der Gon, H.A.C.D., Drouin, A., Elbern, H., Emili, E., Engelen, R.J., Eskes, H.J., Foret, G., Friese, E., Gauss, M., Giannaros, C., Guth, J., Joly, M., Jaumouillé, E., Josse, B., Kadygrov, N., Kaiser, J.W., Krajsek, K., Kuenen, J., Kumar, U., Liora, N., Lopez, E., Malherbe, L., Martinez, I., Melas, D., Meleux, F., Menut, L., Moinat, P., Morales, T., Parmentier, J., Piacentini, A., Plu, M., Poupkou, A., Queguiner, S., Robertson, L., Rouïl, L., Schaap, M., Segers, A., Sofiev, M., Tarasson, L., Thomas, M., Timmermans, R., Valdebenito Van Velthoven, P., Van Versendaal, R., Vira, J., Ung, A., 2015. A regional air quality forecasting system over Europe: the MACC-II daily ensemble production. Geosci. Model Dev. 8, 2777–2813. https://doi.org/10.5194/GMD-8-2777-2015.
- Martínez-Suller, L., Provolo, G., Brennan, D., Howlin, T., Carton, O.T., Lalor, S.T.J., Richards, K.G., 2010. A note on the estimation of nutrient value of cattle slurry using easily determined physical and chemical parameters. Irish J. Agric. Food Res. 49, 93–97
- Menzi, H., Pain, B., Sommer, S.G., 2002. Manure management: The European perspective. In: Proc. 4th Int. Livestock Waste Management Symp. and Technology Expo, pp. 35–44. Penang, Malaysia (Ong, H.K. et Al. (Eds.)). ISBN 983-99519-2-0.
- Misselbrook, T.H., Nicholson, F.A., Chambers, B.J., 2005. Predicting ammonia losses following the application of livestock manure to land. Bioresour. Technol. 96, 159–168. https://doi.org/10.1016/j.biortech.2004.05.004.
- Neumann, K., Elbersen, B.S., Verburg, P.H., Staritsky, I., Pérez-Soba, M., de Vries, W., Rienks, W.A., 2009. Modelling the spatial distribution of livestock in. Europe. Landsc. Ecol. https://doi.org/10.1007/s10980-009-9357-5.
- Nicholson, F.A., Bhogal, A., Chadwick, D., Gill, E., Gooday, R.D., Lord, E., Misselbrook, T., Rollett, A.J., Sagoo, E., Smith, K.A., Thorman, R.E., Williams, J.R., Chambers, B.J., 2013. An enhanced software tool to support better use of manure nutrients: MANNER-NPK. Soil Use Manag. 29, 473–484. https://doi.org/10.1111/ sum\_12078
- Pelster, D.E., Watt, D., Strachan, I.B., Rochette, P., Bertrand, N., Chantigny, M.H., 2019. Effects of initial soil moisture, clod size, and clay content on ammonia volatilization after subsurface band application of urea. J. Environ. Qual. 48, 549–558. https:// doi.org/10.2134/JEQ2018.09.0344.
- Rösemann, C., Haenel, H.-D., Vos, C., Dämmgen, U., Döring, U., Wulf, S., Eurich-Menden, B., Freibauer, A., Döhler, H., Schreiner, C., Osterburg, B., Fu\ss, R., 2021.
   Calculations of gaseous and particulate emissions from German agriculture 1990 2019: Report on methods and data (RMD) Submission 2021; Berechnung von gasund partikelförmigen Emissionen aus der deutschen Landwirtschaft 1990 2019:
   Report zu Methoden u. Johann-Heinrich-von-Thünen-Institut, Braunschweig, Germany. https://doi.org/10.3220/REP1616572444000.
- Schaap, M., Hendriks, C., Kranenburg, R., Kuenen, J., Segers, A., Schlutow, A., Nagel, H. D., Ritter, A., Banzhaf, S., 2018. PINETI-3: Modellierung atmosphärischer Stoffeinträge von 2000 bis 2015 zur Bewertung der ökosystem-spezifischen Gefährdung von Biodiversität durch Luftschadstoffe in Deutschland. Texte Umweltbundesamt 79, 149.
- Schaap, M., Segers, A., Curier, L., Eskes, H., Kumar, U., 2012. LOTOS-EUROS regional forecasting system and performances 36, 1–36.
- Schaap, M., Timmermans, R.M.A., Roemer, M., Boersen, G.A.C., Builtjes, P.J.H., Sauter, F.J., Velders, G.J.M., Beck, J.P., 2008. The LOTOS EUROS model: description, validation and latest developments. Int. J. Environ. Pollut. 32, 270. https://doi.org/10.1504/ijep.2008.017106.

- Shephard, M.W., Cady-Pereira, K.E., 2015. Cross-track Infrared Sounder (CrlS) satellite observations of tropospheric ammonia. Atmos. Meas. Tech. 8, 1323–1336. https:// doi.org/10.5194/AMT-8-1323-2015.
- Shephard, M.W., Dammers, E.E., Cady-Pereira, K.K., Kharol, S., Thompson, J., Gainariu-Matz, Y., Zhang, J.A., McLinden, C., Kovachik, A., Moran, M., Bittman, S.E., Sioris, C., Griffin, D.J., Alvarado, M., Lonsdale, C., Savic-Jovcic, V., Zheng, Q., 2020. Ammonia measurements from space with the Cross-track Infrared Sounder: characteristics and applications. Atmos. Chem. Phys. 20, 2277–2302. https://doi.org/10.5194/ACP-20-2277-2020
- Sintermann, J., Neftel, A., Ammann, C., Häni, C., Hensen, A., Loubet, B., Flechard, C.R., 2012. Are ammonia emissions from field-applied slurry substantially over-estimated in European emission inventories? Biogeosciences 9, 1611–1632. https://doi.org/ 10.5194/BG-9-1611-2012.
- Skjøth, C.A., Geels, C., Berge, H., Gyldenkaerne, S., Fagerli, H., Ellermann, T., Frohn, L. M., Christensen, J., Hansen, K.M., Hansen, K.M., Hertel, O., 2011. Spatial and temporal variations in ammonia emissions ĝ€" a freely accessible model code for Europe. Atmos. Chem. Phys. 11, 5221–5236. https://doi.org/10.5194/acp-11-5221-2011.
- Skjøth, C.A., Hertel, O., Gyldenkaerne, S., Ellermann, T., 2004. Implementing a dynamical ammonia emission parameterization in the large-scale air pollution model ACDEP. J. Geophys. Res. Atmos. 109 https://doi.org/10.1029/2003jd003895 n/a-n/a
- Smith, E., Gordon, R., Bourque, C., Campbell, A., Génermont, S., Rochette, P., Mkhabela, M., 2009. Simulated management effects on ammonia emissions from field applied manure. J. Environ. Manage. 90, 2531–2536. https://doi.org/10.1016/ j.jenyman.2009.01.012.
- Søgaard, H.T., Sommer, S.G., Hutchings, N.J., Huijsmans, J.F.M., Bussink, D.W., Nicholson, F., 2002. Ammonia volatilization from field-applied animal slurry-the ALFAM model. Atmos. Environ. https://doi.org/10.1016/S1352-2310(02)00300-X.
- Sommer, S.G., Schjoerring, J.K., Denmead, O.T., 2004. Ammonia emission from mineral fertilizers and fertilized crops. Adv. Agron. 82, 557–622. https://doi.org/10.1016/ S0065-2113(03)82008-4.
- Sommer, S.G., Webb, J., Hutchings, N.D., 2019. New emission factors for calculation of ammonia volatilization from European livestock manure management systems. Front. Sustain. Food Syst. 3, 101. https://doi.org/10.3389/FSUFS.2019.00101/ BIRTEY
- Sonneveld, M.P.W., Schröder, J.J., Vos, J.A.de, Monteny, G.J., Mosquera, J., Hol, J.M.G., Lantinga, E.A., Verhoeven, F.P.M., Bouma, J., 2008. A whole-farm strategy to reduce environmental impacts of Nitrogen. J. Environ. Qual. 37, 186–195. https://doi.org/ 10.2134/JEQ2006.0434.
- Stokstad, E., 2014. Ammonia pollution from farming may exact hefty health costs. Science 343 (80). https://doi.org/10.1126/science.343.6168.238. 238 LP =238.
- Sutton, M.A., Reis, S., Riddick, S.N., Dragosits, U., Nemitz, E., Theobald, M.R., Tang, Y.S., Braban, C.F., Vieno, M., Dore, A.J., Mitchell, R.F., Wanless, S., Daunt, F., Fowler, D., Blackall, T.D., Milford, C., Flechard, C.R., Loubet, B., Massad, R., Cellier, P., Personne, E., Coheur, P.F., Clarisse, L., Van Damme, M., Ngadi, Y., Clerbaux, C., Skjøth, C.A., Geels, C., Hertel, O., Wichink Kruit, R.J., Pinder, R.W., Bash, J.O., Walker, J.T., Simpson, D., Horváth, L., Misselbrook, T.H., Bleeker, A., Dentener, F., de Vries, W., 2013. Towards a climate-dependent paradigm of ammonia emission and deposition. Philos. Trans. R. Soc. B Biol. Sci. 368, 20130166 https://doi.org/10.1098/rstb.2013.0166.
- Thompson, R.B., Pain, B.F., Rees, Y.J., 1990. Ammonia volatilization from cattle slurry following surface application to grassland: II. Influence of application rate, wind speed and applying slurry in narrow bands. Plant Soil 125, 119–128.
- Truong, A.H., Kim, M.T., Nguyen, T.T., Nguyen, N.T., Nguyen, Q.T., 2018. Methane, nitrous oxide and ammonia emissions from livestock farming in the red river delta, vietnam: an inventory and projection for 2000–2030. Sustain 10, 3826. https://doi.org/10.3390/SU10103826, 2018VolPage 3826 10.
- Umweltbundesamt, 2020. Reported emission data [WWW Document]. URL https://www.ceip.at/webdab-emission-database/reported-emissiondata (accessed 11.15.22).
- van Bruggen, C., de Bode, M.J.C., Evers, A.G., van der Hoek, K.W., Luesink, H.H., van Schijndel, M.W., 2010. Gestandaardiseerde berekeningsmethode voor dierlijke mest en mineralen: standaardcijfers 1990-2008. Centraal Bureau voor de Statistiek.
- van Bruggen, C., Groenestein, C.M., de Haan, B.J., Hoogeveen, M.W., Huijsmans, J.F.M., Sluis, S.M., Velthof, G.L., 2012. Ammonia emissions from animal manure and inorganic fertilisers in 2009: calculated with the Dutch National Emissions Model for Ammonia (NEMA), WOt-werkdocument. Wettelijke Onderzoekstaken Natuur & Milieu.
- Van Damme, M., Clarisse, L., Dammers, E., Liu, X., Nowak, J.B., Clerbaux, C., Flechard, C.R., Galy-Lacaux, C., Xu, W., Neuman, J.A., Tang, Y.S., Sutton, M.A., Erisman, J.W., Coheur, P.F., 2015. Towards validation of ammonia (NH3) measurements from the IASI satellite. Atmos. Meas. Tech. 8, 1575–1591. https://doi. org/10.5194/amt.8-1575-2015.
- Van Damme, M., Clarisse, L., Whitburn, S., Hadji-Lazaro, J., Hurtmans, D., Clerbaux, C., Coheur, P.-F., 2018. Industrial and agricultural ammonia point sources exposed. Nature 564, 99–103. https://doi.org/10.1038/s41586-018-0747-1.
- Van Damme, M., Whitburn, S., Clarisse, L., Clerbaux, C., Hurtmans, D., Coheur, P.-F., 2017. Version 2 of the IASI NH3 neural network retrieval algorithm: near-real-time and reanalysed datasets. Atmos. Meas. Tech. 10, 4905–4914. https://doi.org/ 10.5194/amt-10-4905-2017.
- Velthof, G.L., 2014. Report Task 1 of Methodological studies in the field of Agro-Environmental Indicators. Lot 1 excretion factors Final Draft.
- Velthof, G.L., Oudendag, D., Witzke, H.P., Asman, W.A.H., Klimont, Z., Oenema, O., 2009. Integrated assessment of nitrogen losses from agriculture in EU-27 using

- MITERRA-EUROPE. J. Environ. Qual. 38, 402. https://doi.org/10.2134/
- Velthof, G.L., van Bruggen, C., Groenestein, C.M., de Haan, B.J., Hoogeveen, M.W., Huijsmans, J.F.M., 2012. A model for inventory of ammonia emissions from agriculture in the Netherlands. Atmos. Environ. 46, 248–255. https://doi.org/ 10.1016/j.atmosenv.2011.09.075.
- Wang, Y., Dong, H., Zhu, Z., Gerber, P.J., Xin, H., Smith, P., Opio, C., Steinfeld, H., Chadwick, D., 2017. Mitigating greenhouse gas and ammonia emissions from swine manure management: a system analysis. Environ. Sci. Technol. 51, 4503–4511. https://doi.org/10.1021/acs.est.6b06430.
- Webb, J., Misselbrook, T.H., 2004. A mass-flow model of ammonia emissions from UK livestock production. Atmos. Environ. https://doi.org/10.1016/j. atmosenv.2004.01.023.
- Webb, J., Pain, B., Bittman, S., Morgan, J., 2010. The impacts of manure application methods on emissions of ammonia, nitrous oxide and on crop response—a review. Agric. Ecosyst. Environ. 137, 39–46. https://doi.org/10.1016/J.AGEE.2010.01.001.
- Zavyalov, V., Esplin, M., Scott, D., Esplin, B., Bingham, G., Hoffman, E., Lietzke, C., Predina, J., Frain, R., Suwinski, L., Han, Y., Major, C., Graham, B., Phillips, L., 2013. Noise performance of the CrlS instrument. J. Geophys. Res. Atmos. 118 (13), 120. https://doi.org/10.1002/2013JD020457, 108-13.